NASA TECHNICAL MEMORANDUM

NASA TM X-3384

THRUST PERFORMANCE OF ISOLATED, TWO-DIMENSIONAL SUPPRESSED PLUG NOZZLES WITH AND WITHOUT EJECTORS AT MACH NUMBERS FROM 0 TO 0.45

Douglas E. Harrington, James J. Schloemer, and Stanley A. Skebe

Lewis Research Center
Cleveland, Ohio 44135

NATIONAL AERONAUTICS AND SPACE ADMINISTRATION • WASHINGTON, D. C. • MAY 1976

1. Report No.	2. Government Accession No.	3. Recipient's Catalog No.
NASA TM X-3384		

4. Title and Subtitle	5. Report Date
THRUST PERFORMANCE OF ISOLATED, TWO-DIMENSIONAL SUPPRESSED PLUG NOZZLES WITH AND WITHOUT EJECTORS AT MACH NUMBERS FROM 0 TO 0.45	May 1976
	6. Performing Organization Code
7. Author(s) Douglas E. Harrington, Lewis Research Center; James J. Schloemer, General Electric Co., Cincinnati, Ohio; and Stanley A. Skebe, Lewis Research Center	8. Performing Organization Report No. E-8556
	10. Work Unit No. 505-11
9. Performing Organization Name and Address Lewis Research Center National Aeronautics and Space Administration Cleveland, Ohio 44135	11. Contract or Grant No.
	13. Type of Report and Period Covered Technical Memorandum
12. Sponsoring Agency Name and Address National Aeronautics and Space Administration Washington, D.C. 20546	14. Sponsoring Agency Code

15. Supplementary Notes

16. Abstract

A series of two-dimensional plug nozzles was tested with and without ejector shrouds at free-stream Mach numbers from 0 to 0.45 and over a range of nozzle pressure ratios from 2 to 4. These nozzles were also tested with and without chute noise suppressors. A two-dimensional plug nozzle had an efficiency of 96.1 percent at an assumed takeoff pressure ratio of 3.0 and Mach 0.36. A 12-chute suppressed nozzle with sidewalls had an efficiency of 81.0 percent (15.1 percent below the unsuppressed nozzle).

17. Key Words (Suggested by Author(s))	18. Distribution Statement
Exhaust nozzles; Nozzles; Plug nozzles; Noise suppression; Jet noise; Suppressed nozzles; Two-dimensional nozzles	Unclassified - unlimited STAR Category 07

19. Security Classif. (of this report)	20. Security Classif. (of this page)	21. No. of Pages	22. Price*
Unclassified	Unclassified	36	$4.00

* For sale by the National Technical Information Service, Springfield, Virginia 22161

THRUST PERFORMANCE OF ISOLATED, TWO-DIMENSIONAL SUPPRESSED PLUG NOZZLES WITH AND WITHOUT EJECTORS AT MACH NUMBERS FROM 0 TO 0.45

by Douglas E. Harrington, James J. Schloemer*, and Stanley A. Skebe

Lewis Research Center

SUMMARY

A series of two-dimensional plug nozzles was tested with and without ejector shrouds in the Lewis 8- by 6-Foot Supersonic Wind Tunnel to determine thrust performance at takeoff conditions. These nozzles were also tested with and without chute noise suppressors. The test nozzles were designed primarily for application to advanced supersonic-cruise aircraft in which a dry turbojet or mixed-flow turbofan engine would be used. Data were obtained at free-stream Mach numbers from 0 to 0.45 and nozzle pressure ratios from 2.0 to 4.0.

A two-dimensional baseline plug nozzle had an efficiency of 96.1 percent at an assumed takeoff pressure ratio of 3.0 and Mach 0.36. Efficiency at the assumed takeoff condition was essentially unchanged by the addition of sidewalls to this nozzle. The addition of an ejector to the plug nozzle with sidewalls also had little effect on efficiency, which was 95.8 percent at the takeoff condition. A 12-chute suppressed nozzle with sidewalls had a nozzle efficiency of approximately 81.0 percent (15.1 percent below the baseline nozzle) at the same condition. The addition of an ejector to this configuration reduced the efficiency by approximately 2 percent (to 79.0). The thrust loss of these suppressed nozzles relative to the baseline plug nozzle was due primarily to chute-base pressure drag. For example, at the takeoff condition the 12-chute suppressed nozzle with sidewalls had a chute-base pressure drag of 14 percent of ideal thrust. This performance decrease represents approximately 93 percent of the total thrust loss compared with the baseline plug nozzle. At a nozzle pressure ratio of 3.0, the two-dimensional nozzles were sensitive to external flow. This was particularly true of the 12-chute suppressed nozzles. At Mach 0.36 these nozzles experienced a thrust loss of 4 to 5 percent compared with static performance.

*General Electric Company, Cincinnati, Ohio.

INTRODUCTION

Nozzle concepts appropriate for advanced supersonic cruise aircraft must operate efficiently over a wide range of flight conditions and engine power settings. The axisymmetric and two-dimensional plug nozzle concepts offer the potential of good aerodynamic performance and minimum mechanical complexity. As a consequence, tests have been conducted (e.g., refs. 1 to 14) to optimize the thrust performance, to investigate installation effects, and to determine the heat-transfer characteristics for these types of nozzles.

In recent years increasing emphasis has been placed on the reduction of aircraft noise. During takeoff and climb out, when the aircraft engines are at a high power setting, the dominant noise source is usually associated with the high velocity jet emanating from the exhaust nozzle. Jet noise characteristics for several types of nozzle, including a low-angle conical plug, were evaluated at takeoff pressure ratios in a static test stand (ref. 15). However, takeoff and climb-out speeds associated with advanced supersonic aircraft are relatively high (approximately Mach 0.35). Thus, the effect of flight velocity on jet noise must also be evaluated. Tests to evaluate the effects of flight velocity have been conducted and are reported in references 16 to 19. Several techniques to suppress jet noise are currently under investigation. One concept of interest is the two-dimensional plug nozzle. To suppress noise this nozzle could be configured in an over-the-wing aircraft installation. The wing would then act as a shield to reduce some of the propulsion system noise from the ground during aircraft flyover. To further reduce noise, multiple spoke or chute suppressors could be incorporated in this nozzle concept. After takeoff the suppressor would be retracted and stowed in the two-dimensional plug. However, to properly evaluate a suppressor concept like the multichute, it is necessary to study a tradeoff between high noise suppression and good thrust performance (refs. 20 to 24).

This report presents the thrust performance of a series of two-dimensional plug nozzles tested with and without ejector shrouds in the wind tunnel. These nozzles were also tested with and without chute noise suppressors. The test nozzles were designed primarily for application to advanced supersonic-cruise aircraft in which a dry turbojet or mixed-flow turbofan engine would be used. Data were obtained at free-stream Mach numbers from 0 to 0.45 and nozzle pressure ratios from 2.0 to 4.0. Dry air at approximately the tunnel total temperature (32^{o} C (90^{o} F)) was supplied to the nozzles in this test. The angle of attack of the model was maintained at 0^{o}. The range of Reynolds number was from 8.01×10^{6} to 9.38×10^{6} per meter (2.44×10^{6} to 2.86×10^{6}/ft) at Mach numbers from 0.36 to 0.45, respectively.

APPARATUS AND PROCEDURE

Installation

The test nozzles were strut mounted in the test section of the Lewis 8- by 6-Foot-Supersonic-Wind-Tunnel (ref. 25) as shown in figure 1. The support system consisted of a strut (0° sweep angle) with a thickness to chord ratio of 0.036 and a forebody with a maximum diameter of 21.59 centimeters (8.5 in.). For the test nozzles, which were 16.828 centimeters (6.625 in.) high and 21.896 centimeters (8.656 in.) wide, a transition section was required to mate the 21.59-centimeter (8.5-in.) support forebody diameter to the 16.828- by 21.986-centimeter nozzle cross section. This transition was 2.22 nozzle hydraulic diameters long. Nozzle hydraulic diameter d_h was based on the test nozzle cross-sectional area and perimeter. (See appendix.) A two-dimensional section downstream of the transition was 4.74 nozzle hydraulic diameters long and should have been sufficiently long to reestablish ambient flow conditions. The thrust-minus-drag of the exhaust nozzles was determined from the force- and flow-measuring section located just downstream of the transition section.

The internal geometry of the model showing the details of the force- and flow-measuring section is shown in figure 2. Nozzle weight flow was determined using a choked, long-radius ASME nozzle with a diverging section. Because the metering nozzle was choked, it was necessary to measure only the total pressure and temperature of the airflow. Total pressure P_1 upstream of the flow-metering nozzle was measured using a four-tube, area weighted rake. Total temperature T_1 was measured by two shielded thermocouples. To determine the actual weight flow of the test nozzle, it was necessary to calculate a meter discharge coefficient. In addition, real gas effects were accounted for in the determination of weight flow (ref. 26).

The metric part of the model was cantilevered directly from the diverging section of the flow-metering nozzle (fig. 2). Two strain-gage links were used to measure the axial force between the metric and grounded parts of the model. A flexible seal at the throat of the flow-metering nozzle was used to separate the metric and grounded sections. The actual thrust-minus-drag of a test nozzle was then determined from the momentum entering the throat of the flow-metering nozzle, a balance force obtained from the two strain gage links, and various pressure-area terms. When testing with external flow, the thrust-minus-drag of the test nozzle (calculated by the method just given) was modified to exclude the friction drag on the surface from the metric break to the beginning of the test nozzles. The beginning of the test nozzles was approximately 3.3 nozzle hydraulic diameters upstream of the end of the nozzles (i.e., plug tip).

Downstream of the choked venturi the nozzle airflow passed through a series of choke plates and screens to provide uniform flow at station 7. The station 7 nozzle total pressure P_7 was determined by four two-tube rakes. Nozzle total temperature T_7

was calculated by subtracting the temperature drop between stations 1 and 7 from T_1. This temperature drop, due to Joule-Thomson throttling of a real gas, was calculated using a curve fit of tabulated properties of air from reference 27. The model pressures, except the high total pressure P_1, were determined from a scanner valve system. The pressure P_1 was determined using four individual pressure transducers.

The procedure during a test run was to set a free-stream Mach number and then go through a variation in nozzle pressure ratio. Since, for a given free-stream Mach number, tunnel static pressure was constant, variations in nozzle pressure ratio were obtained by changing nozzle total pressure P_7.

NOZZLE GEOMETRY

The geometric details of the various nozzles tested are presented in figure 3, and pertinent area ratios are listed in table I. Each of these nozzles had a 15° half-angle, two-dimensional plug. The test results of the baseline plug nozzle (see fig. 3(a)) provided a reference with which to compare the other nozzles. The design pressure ratio of this nozzle, based on its internal expansion area ratio, was 3.2. The baseline plug nozzle with sidewalls is shown in figure 3(b). The sidewalls could effectively inhibit sideline jet noise propagation. Figure 3(c) shows the ejector plug nozzle that was tested to determine the effect of the ejector on thrust performance. The ejector had a small-radius leading edge and was parallel to the plug surface. An ejector could be used with this nozzle to promote the mixing of the low-velocity external air with the high-velocity nozzle flow; thus providing a possible reduction in jet noise. In a full-scale version, the sidewalls and ejector could be treated to provide a further reduction in jet noise.

To further investigate techniques for suppressing jet noise, a 12-chute suppressed nozzle was tested with sidewalls (fig. 3(d)). The chutes were installed with their trailing edges oriented normal to the plug surface. The chutes were open and had a V-shaped cross section (view B-B, fig 3(d)). The geometric area ratio $(AR)_{geo}$ of this suppressed nozzle was approximately 2. The geometric area ratio is defined as the ratio of the rectangular flow area with chutes retracted to the geometric flow area with the chutes deployed. As a means of increasing the ventilation region downstream of the chute-exit plane, sidewall slots were opened in the suppressed nozzle to form another nozzle configuration (also shown in fig. 3(d)).

The last two configurations tested were the suppressed ejector nozzle and the suppressed ejector nozzle with sidewall slots. These two models were the same, except for the sidewall slots, and their geometric details are presented in figure 3(e). Both nozzles incorporated all the hardware used in the preceding suppressed nozzles, including the long side plates and the 12-chute suppressor. In addition, the ejector used for the ejector plug nozzle (fig. 3(c)) was used. The position of the ejector shroud relative to

the sidewalls and the plug was the same as that of the ejector plug nozzle.

Instrumentation

Static-pressure instrumentation for the two-dimensional test nozzles is presented in figure 4. The axial reference point (X = 0) for these nozzles (both suppressed and unsuppressed) was located at the maximum height of the plug. Locations of the base pressures of the chutes of the suppressed nozzles are tabulated as a function of the dimensionless height parameter H. Forces on the various nozzle components were determined by a pressure-area integration and do not include friction drag. Ejector instrumentation details for the two-dimensional ejector plug nozzle are shown in figure 5. An attempt was made to estimate the entrained external flow for this configuration using two total-pressure rakes and four static-pressure taps.

RESULTS AND DISCUSSION

Nozzle performance of the two-dimensional plug nozzles (without suppressors) is presented as a function of nozzle pressure ratio in figure 6. The baseline plug nozzle had a nozzle efficiency of 96.1 percent at a takeoff pressure ratio of 3.0 and Mach 0.36 (fig. 6(b)). Efficiency at the takeoff condition was essentially unchanged (96.3 percent) with the addition of sidewalls to the baseline nozzle. The addition of an ejector to the plug nozzle with sidewalls also had little effect on efficiency, which was 95.8 percent at the takeoff condition. For static conditions (fig. 6(a)) the ejector plug nozzle had the highest nozzle efficiencies at pressure ratios less than 3.0. The peak efficiency of this configuration was 97.9 percent at a nozzle pressure ratio of 2.5. However, with external flow (figs. 6(b) - (d)) the ejector plug nozzle generally had lower performance than either of the other two plug nozzle configurations at pressure ratios less than 3.

Over the Mach number range investigated the level and shape of the nozzle efficiency curves for the plug nozzle with and without sidewalls were the same through a nozzle pressure ratio of 3.0. Between nozzle pressure ratios of 3.0 and 3.5, the addition of sidewalls reduced nozzle efficiency 1 to 1.6 percent. But the plug nozzle with sidewalls recovered to a nozzle efficiency level equal to or greater than that of the baseline plug nozzle at a nozzle pressure ratio of 4.0.

Nozzle efficiencies of the 12-chute suppressed nozzles, with and without an ejector shroud and sidewall slots, are presented with the efficiency of the baseline plug as a function of nozzle pressure ratio in figure 7. The efficiency curves of the four sup-

pressed configurations monotonically increased with nozzle pressure ratio. The suppressed nozzle with sidewalls had the highest nozzle efficiency of the four suppressor configurations. At the takeoff condition (fig. 7(b)) this nozzle had an efficiency of 81.0 percent. The addition of an ejector reduced efficiency by approximately 2 percent (to 79.0). These efficiencies represent a decrease in nozzle performance of 15.1 and 17.1 percent, respectively, compared with the baseline plug nozzle. At the takeoff condition the addition of slots in the sidewalls of the 12-chute suppressed nozzles had relatively little effect on efficiency. For example, the opening of the sidewall slots in the suppressed nozzle with sidewalls (no ejector) caused a reduction in efficiency of approximately 0.6 percent (to 80.4).

The integrated plug pressure forces for the plug nozzle configurations without suppressors are presented in figure 8. The pressure integration extended from the throat to the trailing edge of the plug; the resulting thrust component is presented as a fraction of nozzle ideal thrust. The plug thrust component for the baseline plug nozzle (fig. 8(a)) was insensitive to Mach number and amounted to approximately 2 percent of ideal thrust at pressure ratios above 2.5.

Adding the sidewalls (fig. 8(b)) and the ejector (fig. 8(c)) made the nozzle more sensitive to external flow and reduced the plug thrust at pressure ratios above 2.5. In addition, the nozzle plug force for the ejector plug nozzle was negative (a drag). But it can be inferred from the relatively high nozzle efficiency for this nozzle (fig. 6) that a favorable ejector action must have occurred.

The chute-base pressure drag, as a fraction of nozzle ideal thrust, for the suppressed nozzle with and without the ejector shroud and sidewall slots are presented in figure 9. This nozzle thrust loss was reduced significantly with increasing nozzle pressure ratio. However, this reduction was due primarily to increasing nozzle ideal thrust rather than decreasing chute-base pressure drag (as will be verified in a later figure). The thrust loss of these suppressed nozzles relative to the baseline plug nozzle was due primarily to chute-base pressure drag. For example, at the assumed takeoff condition the 12-chute suppressed nozzle with sidewalls had a chute-base pressure drag of 14 percent of ideal thrust (fig. 9(a)). This performance loss represents approximately 93 percent of the total thrust loss when compared with the baseline plug nozzle. The addition of the ejector shroud to the suppressed nozzle with sidewalls (fig. 9(c)) increased the chute-base pressure loss to 17.4-percent of ideal thrust at the takeoff condition. As might be expected from the results of figure 7, the addition of slots to the sidewalls of these nozzles had little or no effect on chute-base pressure drag (figs. 9(b) and (d)).

In figure 10 the effect of external flow on nozzle efficiency at the takeoff pressure ratio of 3 is presented. Nozzle efficiency for the plug nozzles (without suppressors) was sensitive to external flow, and at Mach 0.36 these nozzles experienced a thrust loss of approximately 1 to 2 percent when compared with their static performance (fig. 10(a)). The 12-chute suppressed nozzles were more sensitive to external flow than their unsup-

pressed counterparts (fig. 10(b)). At Mach 0.36 the suppressed nozzles experienced a thrust loss of 4 to 5 percent when compared with their static performance.

Entrained ejector flow rate was measured for the ejector plug nozzle and is presented in figure 11 as a function of primary nozzle pressure ratio. The entrained flow parameter is defined as the ratio of entrained flow to primary flow. Statically, the entrained flow rate was approximately 11.5 percent of the primary flow in the nozzle pressure ratio range from 3.0 to 4.0. At the takeoff condition the entrained flow ratio was about 23 percent.

Mean nozzle discharge coefficients of the two-dimensional test nozzles are presented in figure 12 as a function of nozzle pressure ratio. Standard deviation was calculated and then used to develop a 95-percent confidence band.

For the plug nozzles (without suppressor, fig. 12(a)) the scatter in discharge coefficient was on the order of ±0.5 percent at the confidence level of 95 percent. In addition to the random scatter in the discharge coefficient, the mean discharge coefficient increased approximately 0.5 percent over the nozzle pressure ratio range of 2 to 4. It is believed that this occurred because of an increase in nozzle geometric throat area A_8 at the higher pressure levels, thus causing an error in the calculated ideal mass flow. However, this error in no way affects the validity of the nozzle thrust data presented. Nozzle efficiencies were based on measured nozzle mass flow, which was determined by using the choked metering nozzle at station 1.

For the 12-chute suppressed nozzles (fig. 12(b)) the scatter in discharge coefficient was on the order of ±1.1 percent at the confidence level of 95 percent. In addition to the random scatter in the discharge coefficient of the suppressed configurations, the mean discharge coefficient increased approximately 1 percent over the nozzle pressure ratio range of 2 to 4.

Internal and external static pressure distributions are presented in figures 13 to 15. Distributions are shown at pertinent Mach numbers and nozzle pressure ratios. Of particular interest are the chute-base pressure distributions presented in figure 15. For all configurations tested chute-base pressure drag levels were about the same at nozzle pressure ratios of 2 and 4. This would seem to verify the discussion of figure 9, which pointed out that the reduction in chute-base drag (as a fraction of nozzle ideal thrust) was due primarily to an increase in ideal thrust with increasing pressure ratio.

SUMMARY OF RESULTS

A series of two-dimensional plug nozzles was tested with and without ejector shrouds in the Lewis 8- by 6-Foot-Supersonic-Wind-Tunnel to determine thrust performance at takeoff conditions. These nozzles were also tested with and without the chute noise suppressors. The test nozzles were designed primarily for application to

advanced supersonic-cruise aircraft in which a dry turbojet or mixed-flow turbofan engine would be used. Data were obtained at free-stream Mach numbers from 0 to 0.45 and nozzle pressure ratios from 2.0 to 4.0. Dry air at approximately tunnel total temperature (32° C (90° F)) was supplied to the nozzles in this test. The following results were obtained:

1. A two-dimensional baseline plug nozzle had a nozzle efficiency of 96.1 percent at an assumed takeoff pressure ratio of 3.0 and at Mach 0.36. Efficiency at the takeoff condition was essentially unchanged with the addition of sidewalls to this nozzle. The addition of an ejector to the plug nozzle with sidewalls also had little effect on efficiency, which was 95.8 percent at the takeoff condition.

2. A 12-chute suppressed nozzle with sidewalls had a nozzle efficiency of approximately 81.0 percent at the takeoff condition. The addition of an ejector reduced the efficiency by approximately 2 percent (to 79.0). These efficiencies represent a decrease in nozzle performance of 15.1 percent and 17.1 percent, respectively, compared with the baseline plug nozzle.

3. The thrust loss of these suppressed nozzles relative to the baseline plug nozzle was due primarily to chute-base pressure drag. For example, at the takeoff condition the 12-chute suppressed nozzle with sidewalls had a chute-base pressure drag of 14 percent of ideal thrust. This performance decrease represents approximately 93 percent of the total thrust loss when compared with the baseline plug nozzle.

4. The addition of slots in the sidewalls of the 12-chute suppressed nozzles had relatively little effect on efficiency at the takeoff condition.

5. At the takeoff nozzle pressure ratio of 3.0, the two-dimensional nozzles were sensitive to external flow. This was particularly true of the 12-chute suppressed nozzles. At Mach 0.36 these nozzles experienced a thrust loss of 4 to 5 percent when compared with static performance.

Lewis Research Center,
National Aeronautics and Space Administration,
Cleveland, Ohio, December 30, 1975,
505-11.

APPENDIX - SYMBOLS

A	cross-sectional or projected area
$(AR)_{eff}$	effective area ratio; ratio of annular flow area with chutes retracted to effective flow area with chutes deployed
$(AR)_{geo}$	geometric area ratio; ratio of annular flow area with chutes retracted to geometric flow area with chutes deployed
C_{D8}	nozzle discharge coefficient
C_p	pressure coefficient, $(p - p_0)/q_0$
D	pressure drag
D_t	total external drag (viscous and pressure)
d	diameter
d_h	hydraulic diameter, 4(cross-sectional area of nozzle/perimeter of nozzle)
F	nozzle gross thrust
$F_{p\ell}$	plug axial force
$(F - D_t)/F_i$	nozzle efficiency
H	height parameter, $(h - h_{p\ell})/(h_{sh} - h_{p\ell})$
h	vertical distance measured from bottom surface of plug
$h_{p\ell}$	vertical distance measured from bottom surface of plug to top surface of plug at nozzle geometric throat (X = 0)
h_{sh}	vertical distance measured from bottom surface of plug to outer-shroud internal surface at nozzle geometric throat (X = 0)
L	plug length; measured downstream from maximum height of plug
M	Mach number
P	total pressure
p	static pressure
q	dynamic pressure
T	total temperature
V	velocity
W_e	entrained mass flow rate (due to ejector pumping)
W_8	nozzle mass flow rate

X axial distance downstream of plug maximum height

Z_e distance normal to two-dimensional ejector shroud

Subscripts:

ch chute

i ideal (based on actual weight flow)

m model

pl plug

sh shroud

t total

β boattail

0 free stream

1 flow-measuring station

7 nozzle-inlet station

8 nozzle-throat station

REFERENCES

1. Bresnahan, Donald L.; and Johns, Albert L.: Cold Flow Investigation of a Low Angle Turbojet Plug Nozzle with Fixed Throat and Translating Shroud at Mach Numbers from 0 to 2.0. NASA TM X-1619, 1968.
2. Wasko, Robert A.; and Harrington, Douglas E.: Performance of a Collapsible Plug Nozzle Having Either Two-Position Cylindrical or Variable Angle Floating Shrouds at Mach Numbers from 0 to 2.0. NASA TM X-1657, 1968.
3. Bresnahan, Donald L.: Experimental Investigation of a 10^{o} Conical Turbojet Plug Nozzle with Translating Primary and Secondary Shrouds at Mach Numbers from 0 to 2.0. NASA TM X-1777, 1969.
4. Johns, Albert L.: Quiescent-Air Performance of a Truncated Turbojet Plug Nozzle with Shroud and Plug Base Flows from a Common Source. NASA TM X-1807, 1969.
5. Harrington, Douglas E.: Performance of a 10^{o} Conical Plug Nozzle with Various Primary Flap and Nacelle Configurations at Mach Numbers from 0 to 1.97. NASA TM X-2086, 1971.
6. Harrington, Douglas E.: Performance of Convergent and Plug Nozzles at Mach Numbers from 0 to 1.97. NASA TM X-2112, 1970.
7. Huntley, Sidney C.; and Samanich, Nick E.: Performance of a 10^{o} Conical Plug Nozzle Using a Turbojet Gas Generator. NASA TM X-52570, 1969.
8. Samanich, Nick E.; and Chamberlin, Roger: Flight Investigation of Installation Effects on a Plug Nozzle Installed on an Underwing Nacelle. NASA TM X-2295, 1971.
9. Jeracki, Robert J.; and Chenoweth, Francis C.: Coolant Flow Effects on the Performance of a Conical Plug Nozzle at Mach Numbers from 0 to 2.0. NASA TM X-2076, 1970.
10. Chenoweth, Francis C.; and Lieberman, Arthur: Experimental Investigation of Heat-Transfer Characteristics of a Film-Cooled Plug Nozzle with Translating Shroud. NASA TN D-6160, 1971.
11. Clark, John S.; and Lieberman, Arthur: Thermal Design Study of an Air-Cooled Plug-Nozzle System for a Supersonic-Cruise Aircraft. NASA TM X-2475, 1972.
12. Johns, Albert L.; and Jeracki, Robert J.: Preliminary Investigation of Performance of a Wedge Nozzle Applicable to a Supersonic-Cruise Aircraft. NASA TM X-2169, 1971.

13. Johns, Albert L.: Flight Investigation of Installation Effects on a Wedge Nozzle Installed on an Underwing Nacelle. NASA TM X-3207, 1975.

14. Maiden, Donald L.: Performance of an Isolated Two-Dimensional Variable-Geometry Wedge Nozzle with Translating Shroud and Collapsing Wedge at Speeds up to Mach 2.01. NASA TN D-7906, 1975.

15. Darchuk, George V.; and Balombin, Joseph R.: Noise Evaluation of Four Exhaust Nozzles for Afterburning Turbojet Engine. NASA TM X-2014, 1970.

16. Burley, R. R.; and Karabinus, R. J.: Flyover and Static Tests to Investigate External Flow Effect on Jet Noise For Non-Suppressor and Suppressor Exhaust Nozzles. AIAA Paper 73-190, Jan. 1973.

17. Burley, Richard R.; and Johns, Albert L.: Flight Velocity Effects on Jet Noise of Several Variations of a Twelve-Chute Suppressor Installed on a Plug Nozzle. NASA TM X-2918, 1974.

18. Burley, Richard R.; and Head, Verlon L.: Flight Velocity Effects on the Jet Noise of Several Variations of a 48-Tube Suppressor Installed on a Plug Nozzle. NASA TM X-2919, 1974.

19. Chamberlin, Roger: Flyover and Static Tests to Study Flight Velocity Effects on Jet Noise of Suppressed and Unsuppressed Plug Nozzle Configurations. NASA TM X-2856, 1973.

20. Breshnahan, Donald L.: Internal Performance of a 10^{o} Conical Plug Nozzle with a Multispoke Primary and Translating External Shroud. NASA TM X-2573, 1972.

21. Johns, Albert L.: Internal Performance of a Wedge Nozzle for a Supersonic-Cruise Aircraft with a Multispoke Primary for Noise Suppression. NASA TM X-2689, 1973.

22. Brausch, J. F.: Flight Velocity Influence of Jet Noise of Conical Ejector, Annular Plug and Segmented Suppressor Nozzles. (General Electric Co.; NAS3-15773), NASA CR-120961, 1972.

23. Harrington, Douglas E.; and Schloemer, James J.: Thrust Performance of Isolated Plug Nozzles with Two Types of 40-Spoke Noise Suppressors at Mach Numbers from 0 to 0.45. NASA TM X-2951, 1974.

24. Harrington, Douglas E.; Schloemer, James J.; and Skebe, Stanley A.: Thrust Performance of Isolated 36-Chute Suppressor Plug Nozzles With and Without Ejectors at Mach Numbers from 0 to 0.45. NASA TM X-3298, 1975.

25. Swallow, Robert J.; and Aiello, Robert A.: NASA Lewis 8 by 6 Foot Supersonic Wind Tunnel. NASA TM X-71542, 1974.

26. Johnson, Robert C.: Real-Gas Effects in Critical-Flow-Through Nozzles and Tabulated Thermodynamic Properties. NASA TN D-2565, 1965.

27. Hilsenrath, Joseph, et al.: Tables of Thermal Properties of Gases. Circ. 564, National Bureau of Standards, 1955.

TABLE I. - PERTINENT AREA RATIOS[a]

Nozzle	A_β/A_m (b)	A_8/A_m	A_{ch}/A_m	A_{pl}/A_m	$(AR)_{geo}$	$(AR)_{eff}$	C_{D8} (nominal)
Two-dimensional baseline plug nozzle	0.084	0.293	-----	0.650	----	----	0.970
Two-dimensional baseline plug nozzle with sidewalls, and ejector plug nozzle	.119	.293	-----	.616	----	----	.970
All 12-chute suppressed nozzles	.074	.191	0.188	.554	2.02	2.07	.975

[a]All areas are projected on a plane normal to the nozzle axis (except A_8, which is the actual geometric throat area).

[b]A_β includes sidewall boattail area but not ejector boattail area.

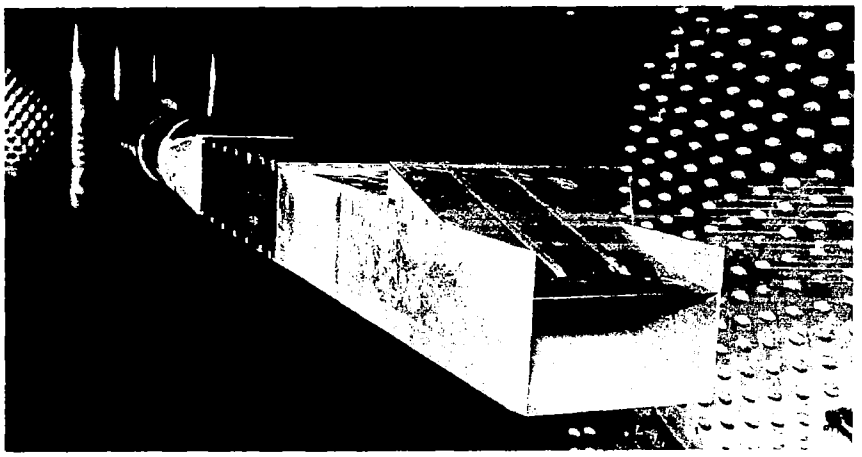

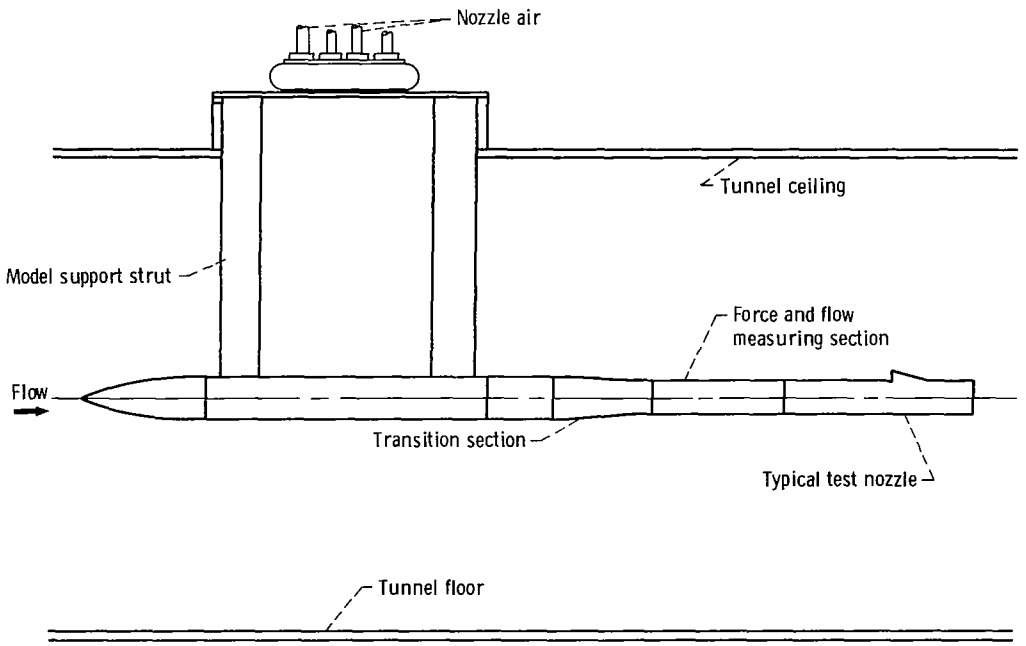

Figure 1. - Model installed in 8- by 6-Foot Supersonic Wind Tunnel.

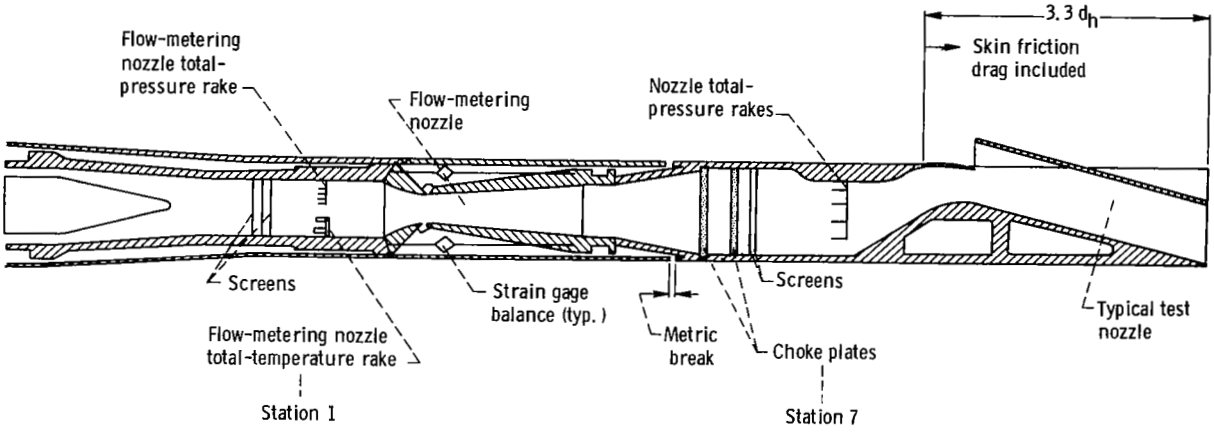

Figure 2. - Model internal geometry and thrust measuring system.

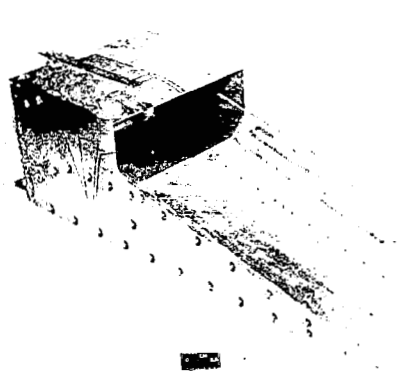

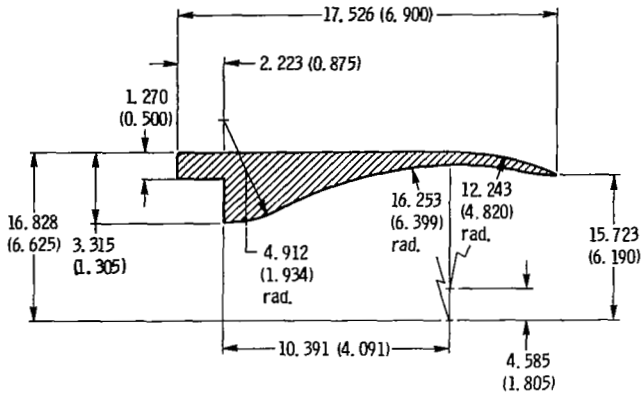

Detail A

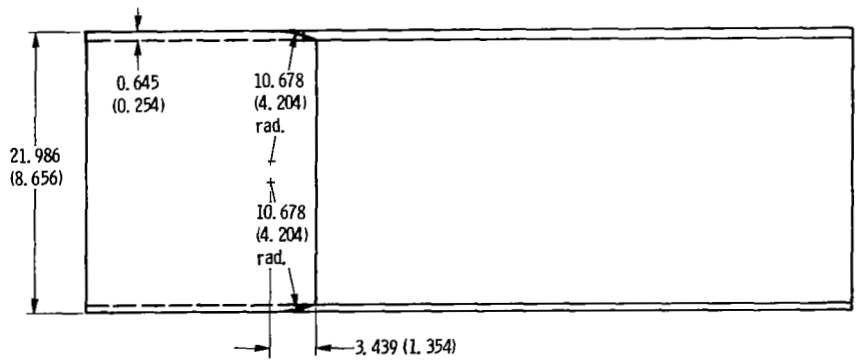

Top view

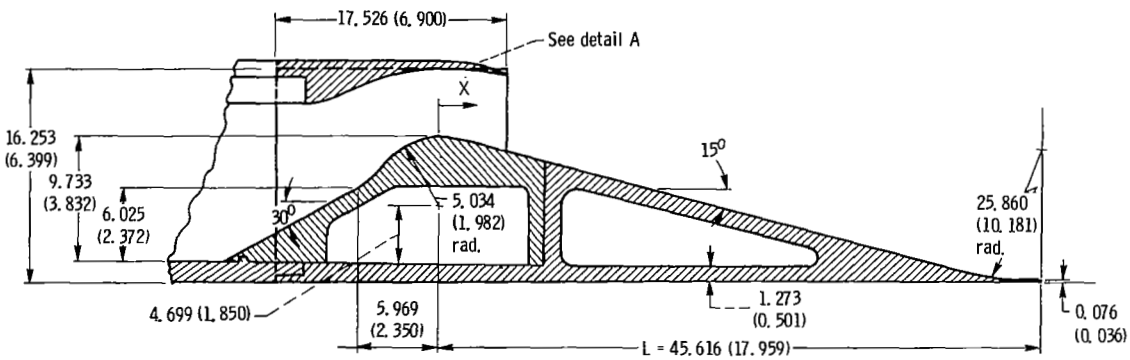

(a) Baseline plug nozzle. Note: Detail A also applies to plug nozzle with sidewalls and ejector plug nozzle (pts. (b) and (c)).

Figure 3. - Geometric details of the two-dimensional plug nozzles (without suppressors). (All dimensions are in cm (in.).)

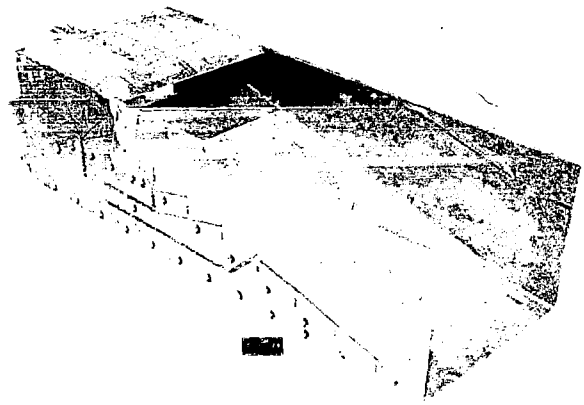

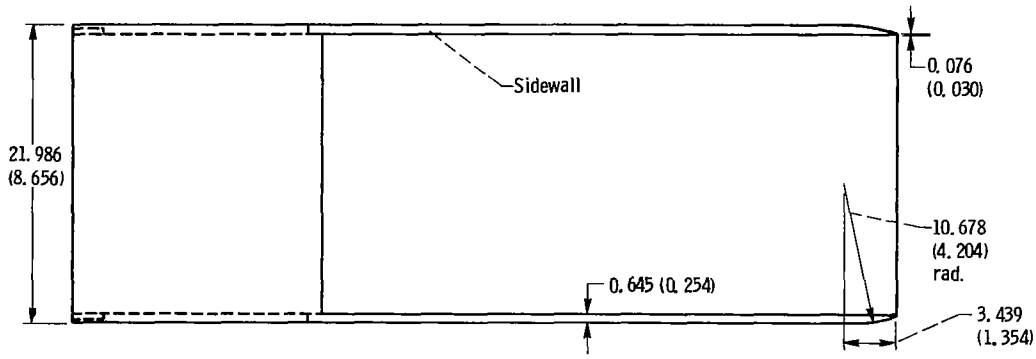

Top view

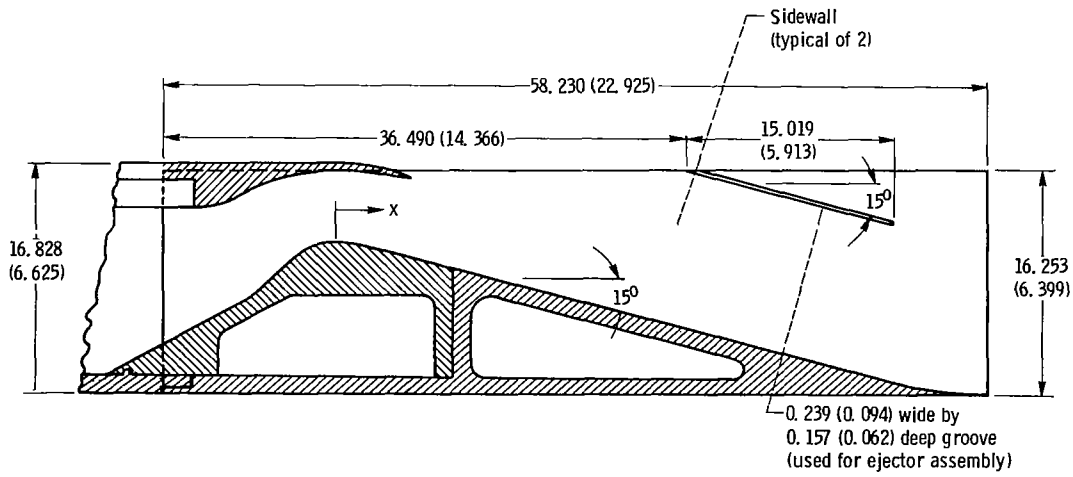

(b) Plug nozzle with sidewalls.

Figure 3. - Continued.

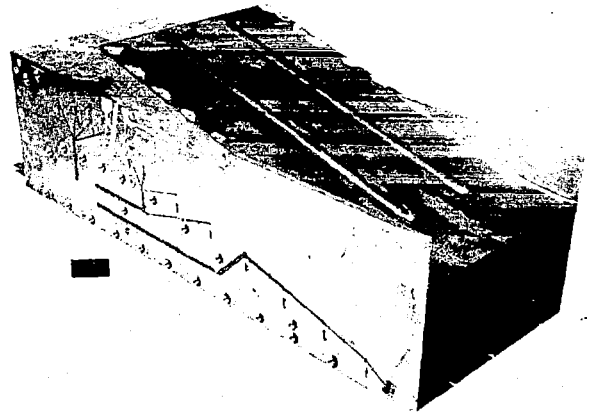

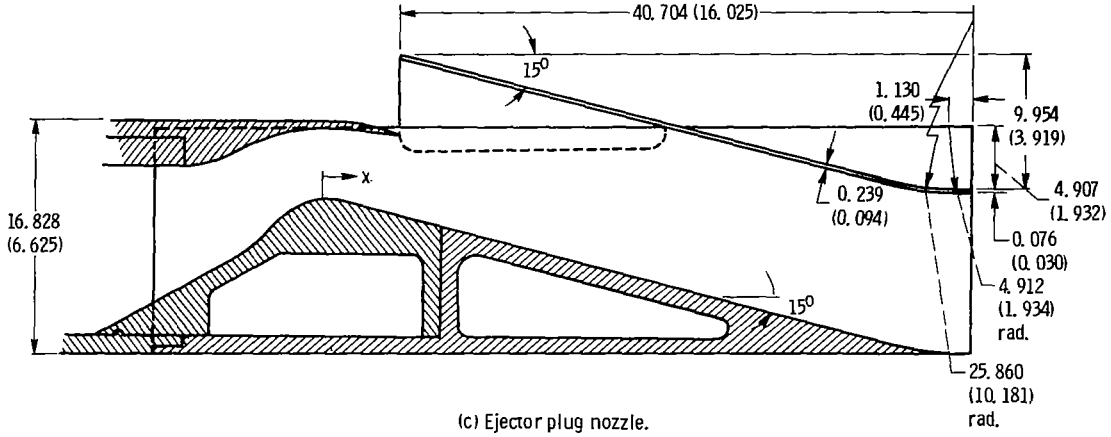

(c) Ejector plug nozzle.

Figure 3. - Continued

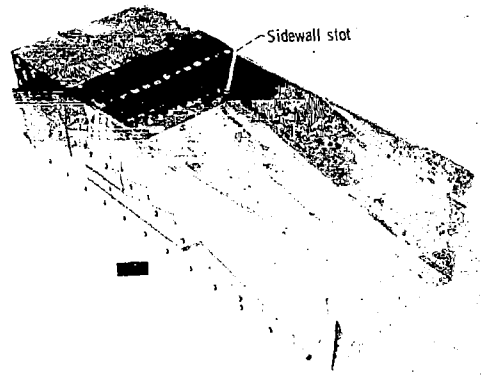

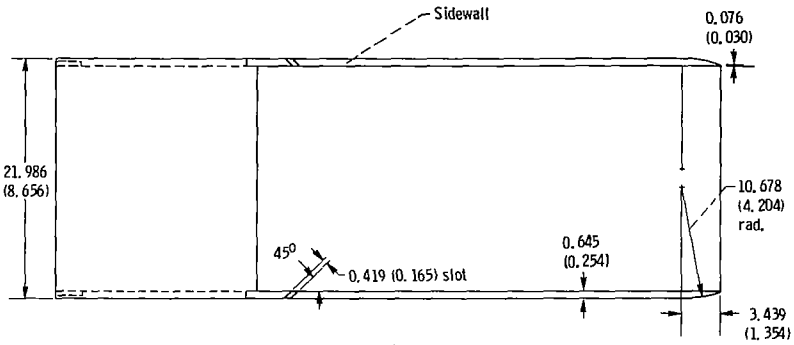

Top view

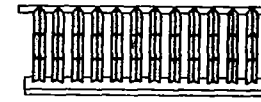

Section A-A

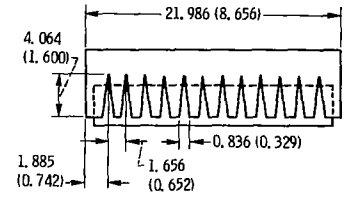

Section B-B.

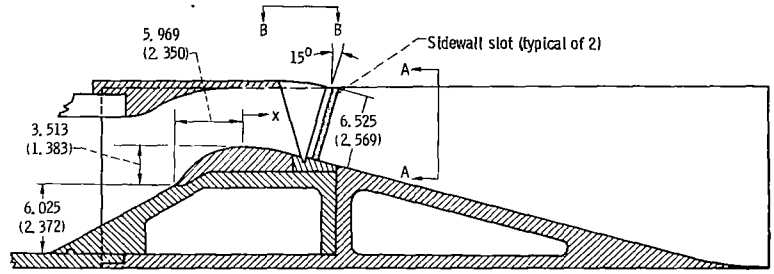

With sidewall slots

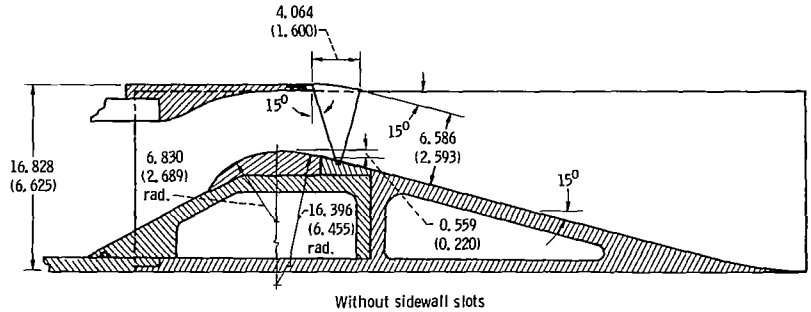

Without sidewall slots

(d) 12-Chute suppressed nozzle with sidewalls (with and without sidewall slots).

Figure 3. - Continued.

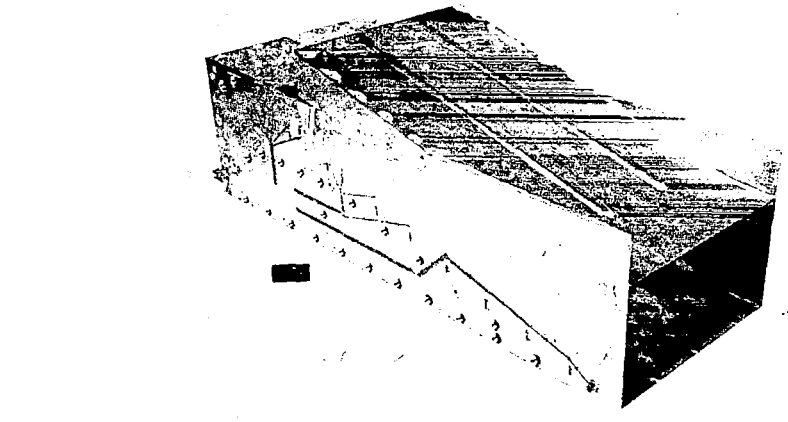

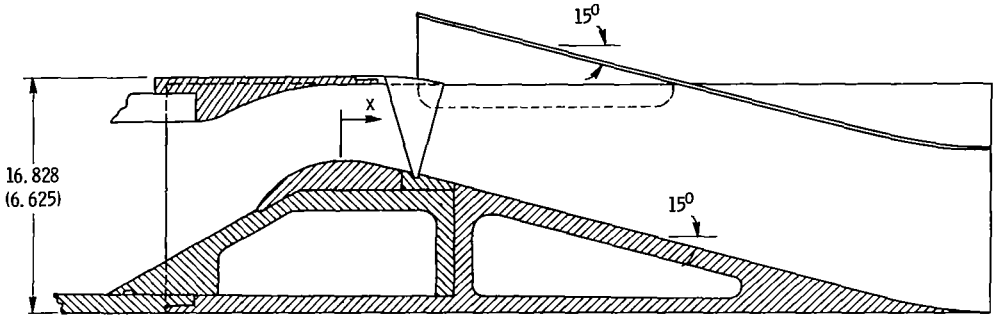

(e) 12-Chute suppressed ejector nozzle with and without sidewall slots. (Note: See pt. (d) for sidewall-slot details.)

Figure 3. - Concluded.

Orifice	Orifice location		Type of pressure	Orifice	Orifice location		Type of pressure
	x/L	y/L			x/L	y/L	
1	-0.215	0.227	External	35	0	0.241	Plug
2	-.054	.227	shroud	36	.031	.363	
3	0	.227		37	.031	.241	
4	.054	.227		38	.084	.241	
5	.081	.363		39	.108	.119	
6	.081	.227		40	.108	.241	
7	.097	.255		41	.193	.241	
8	.102	.119		42	.246	.363	
9	.108	.084		43	.246	.241	
10	.108	.241		44	.300	.241	
11	-.108	.241	Internal	45	.354	.119	
12	-.054	.241	shroud	46	.354	.241	
13	0	.363		47	.408	.241	
14	0	.241		48	.462	.363	
15	.054	.241		49	.462	.241	
16	-.077	.014	Sidewall[a]	50	.516	.241	
17	0			51	.569	.119	
18	.058			52	.569	.241	
19	.107			53	.623	.241	
20	.192			54	.677	.363	
21	.246			55	.677	.241	
22	.354			56	.731	.241	
23	.462			57	.785	.119	
24	.569			58	.785	.241	
25	.677			59	.839	.241	
26	.785			60	.893	.363	
27	.893			61	.893	.241	
28	1.000			62	.946	.241	
29	-0.185	.241	Plug	63	1.000	.119	
30	-.131	.241		64	1.000	.241	
31	-.077	.241					
32	-.023	.363					
33	-.023	.241					
34	0	.119					

[a]Orifices 20 to 28 do not apply to the baseline plug nozzle.

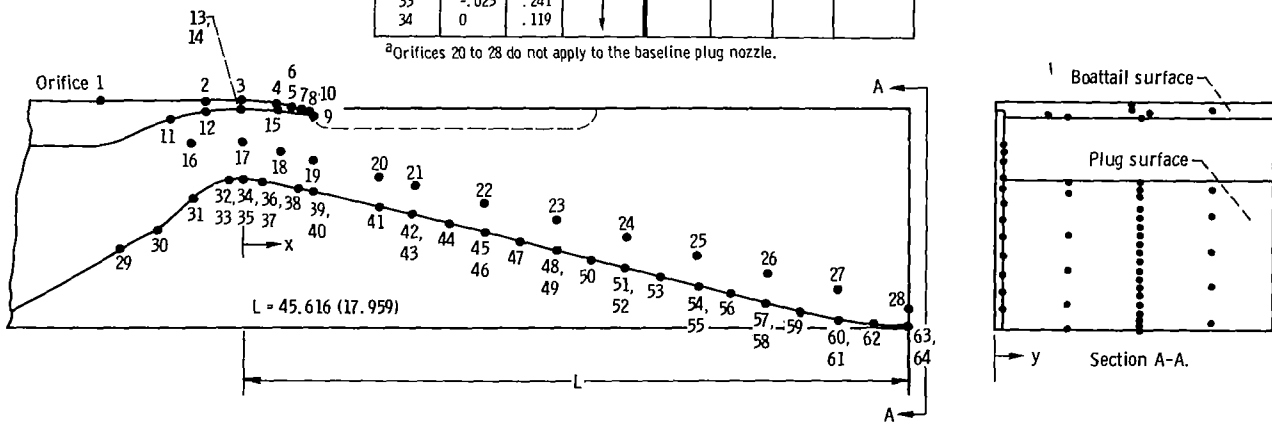

(a) Two-dimensional plug nozzles.

Figure 4. - Static-pressure instrumentation for two-dimensional nozzles.

Orifice	Orifice location		Type of pressure	Orifice	Orifice location		Type of pressure
	x/L	y/L			x/L	y/L	
1	0.108	0.060	External shroud	24	0.246	0.363	Plug
2	.108	.241		25	.246	.241	
3	.159	.060		26	.300	.241	
4	.159	.241		27	.354	.119	
5	-.077	.014	Sidewall	28	.354	.241	
6	0			29	.408	.241	
7	.058			30	.462	.363	
8	.107			31	.462	.241	
9	.192			32	.516	.241	
10	.246			33	.569	.119	
11	.354			34	.569	.241	
12	.462			35	.623	.241	
13	.569			36	.677	.363	
14	.677			37	.677	.241	
15	.785			38	.731	.241	
16	.893			39	.785	.119	
17	1.000			40	.785	.241	
18	.122	.241	Plug	41	.839	.241	
19	.129	.241		42	.893	.363	
20	.129	.018		43	.893	.241	
21	.149	.241		44	.946	.241	
22	.149	.116		45	1.000	.119	
23	.193	.241		46	1.000	.241	

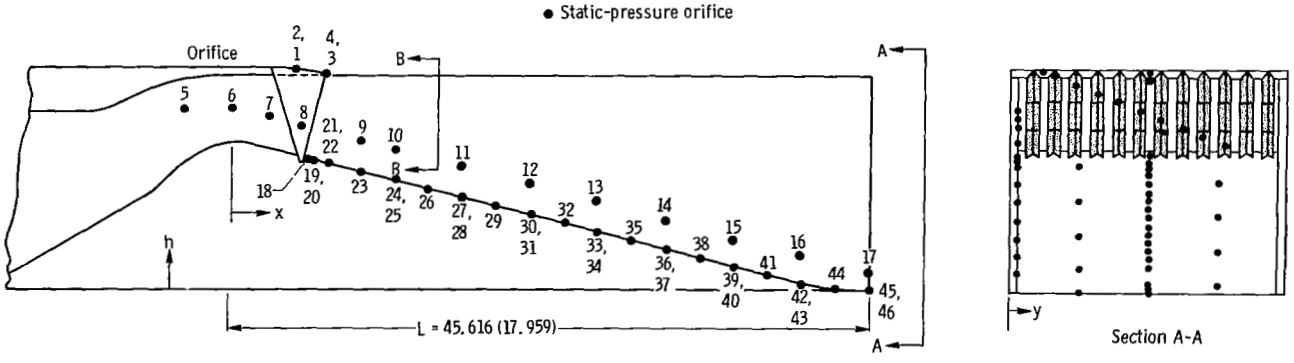

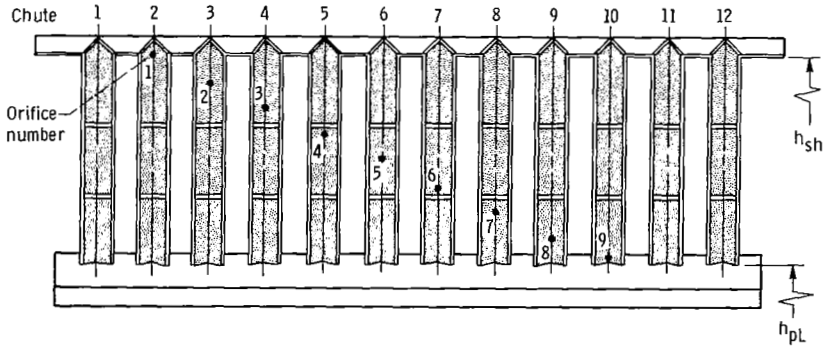

Chute-base static pressures		
Orifice	Chute	Height parameter, H
1	2	1.000
2	3	.875
3	4	.750
4	5	.626
5	6	.501
6	7	.376
7	8	.252
8	9	.127
9	10	.004

View B-B. Chute-base static pressures.
(b) Suppressed nozzles.

Figure 4. - Concluded.

Tube	Distance from ejector, Z_e	
	cm	in.
1	0.33	0.13
2	1.50	.59
3	2.67	1.05
4	3.81	1.50
5	4.98	1.96

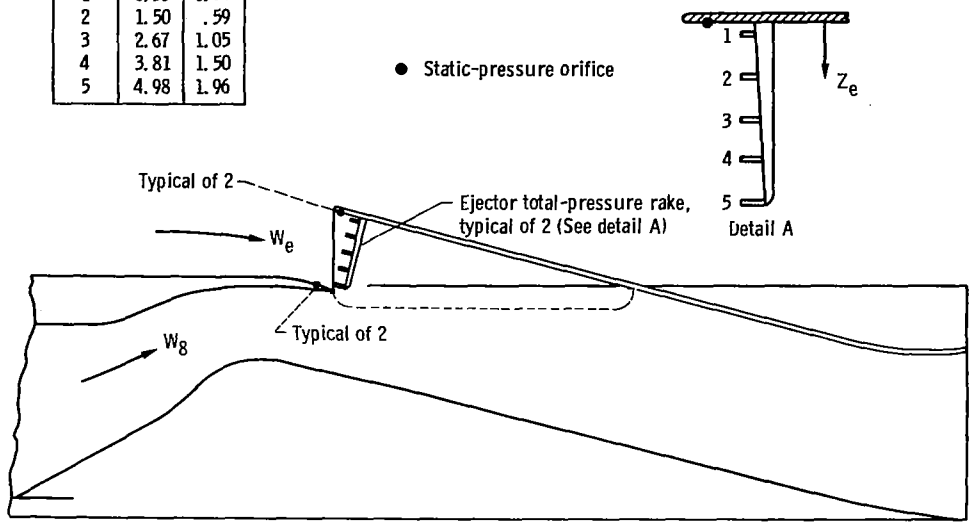

Figure 5. - Ejector instrumentation for ejector plug nozzle.

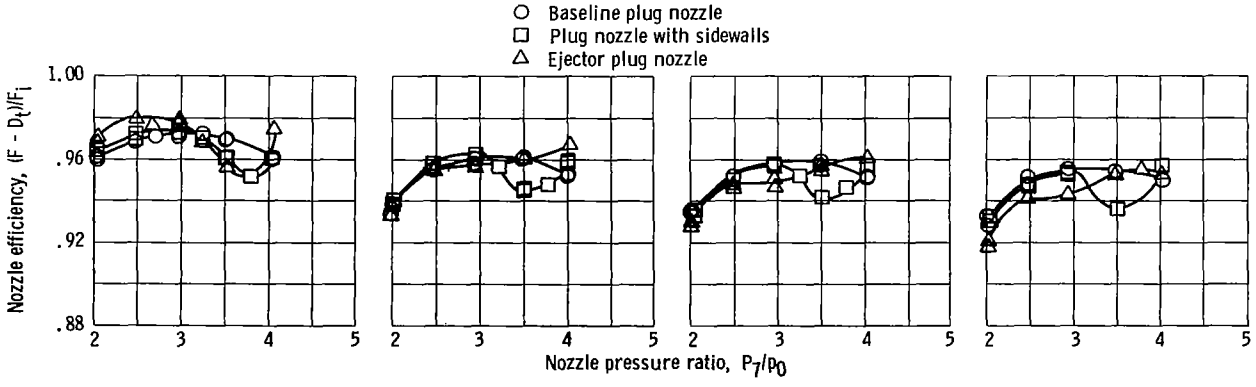

(a) Free-stream Mach number, 0. (b) Free-stream Mach number, 0.36. (c) Free-stream Mach number, 0.40. (d) Free-stream Mach number, 0.45.

Figure 6. - Comparison of performance of two-dimensional plug nozzles without suppressors.

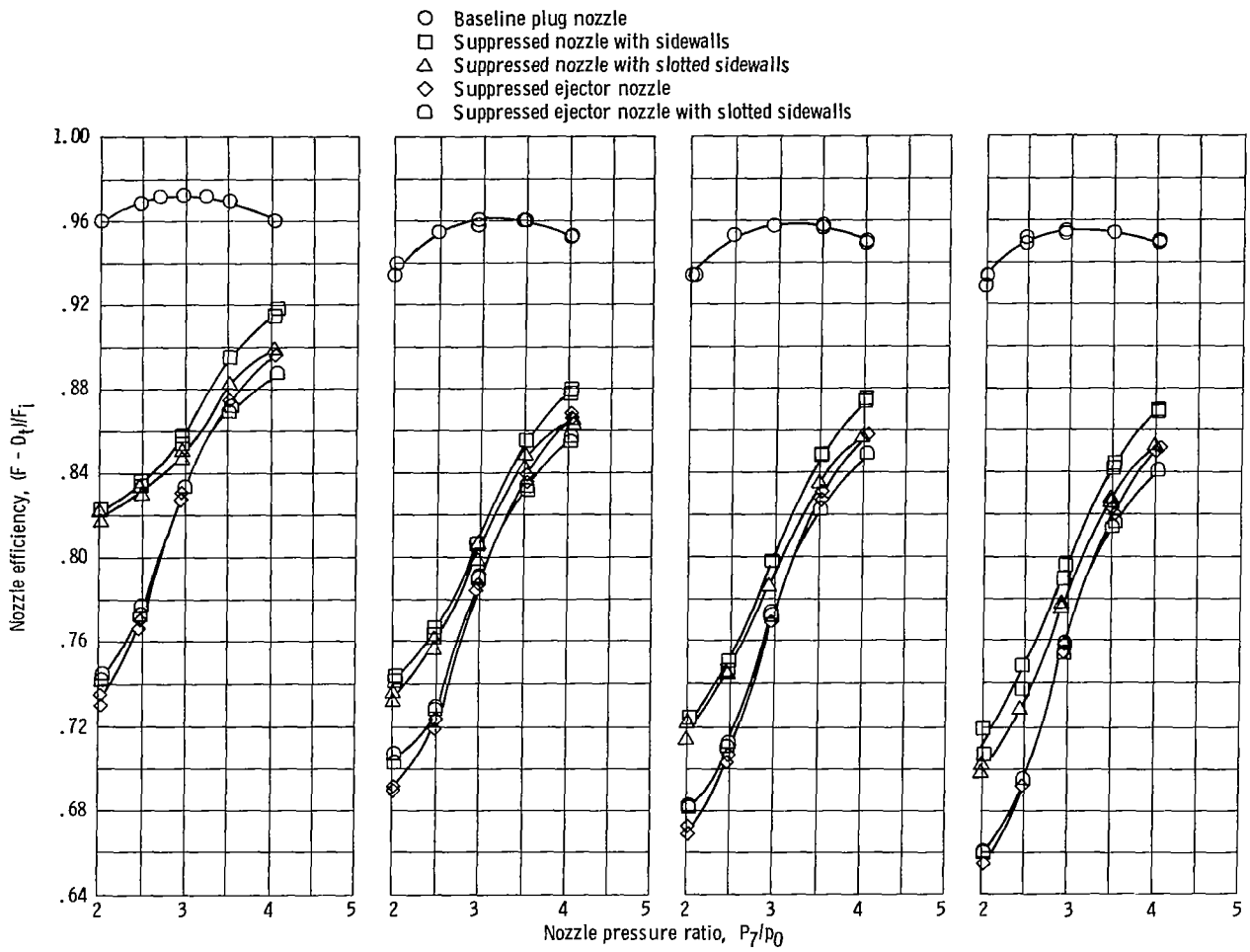

(a) Free-stream Mach number, 0. (b) Free-stream Mach number, 0.36. (c) Free-stream Mach number, 0.40. (d) Free-stream Mach number, 0.45.

Figure 7. - Comparison of performance for baseline plug nozzle and 12-chute suppressed nozzles.

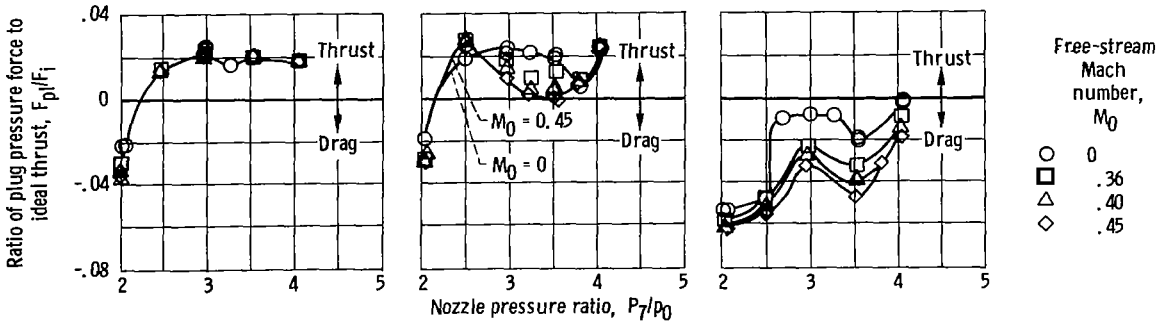

(a) Baseline plug nozzle. (b) Plug nozzle with sidewalls. (c) Ejector plug nozzle.

Figure 8. - Plug pressure force for two-dimensional plug nozzles without suppressors.

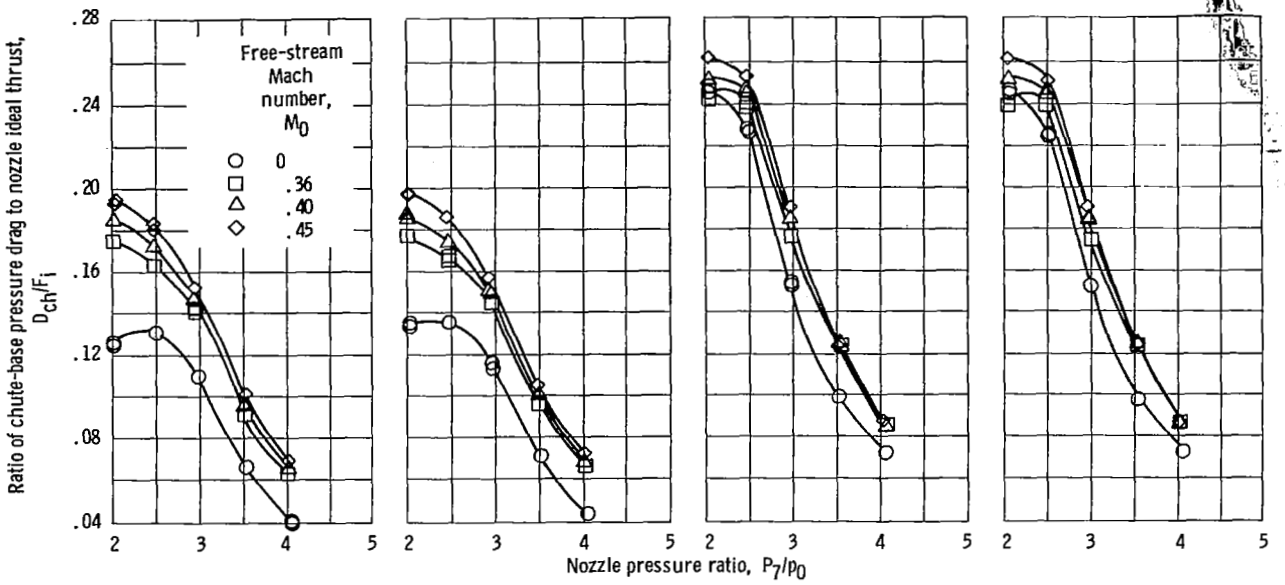

(a) Suppressed nozzle with sidewalls.

(b) Suppressed nozzle with slotted sidewalls.

(c) Suppressed ejector nozzle.

(d) Suppressed ejector nozzle with slotted sidewalls.

Figure 9. - Nozzle thrust loss from chute-base pressure drag for 12-chute suppressed nozzles.

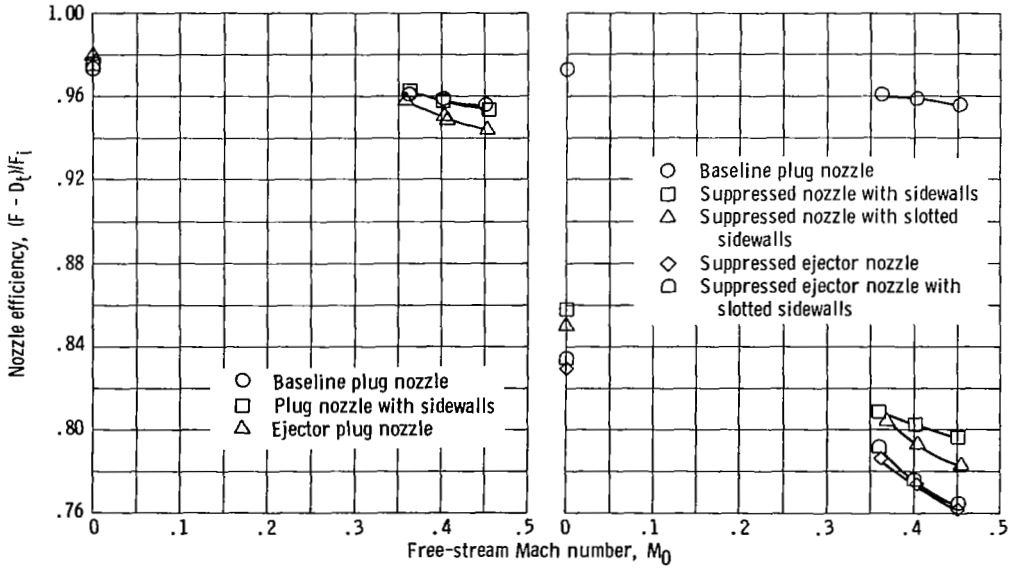

(a) Plug nozzles without suppressors.

(b) 12-Chute suppressed nozzles.

Figure 10. - External flow effects on two-dimensional nozzle performance. Nozzle pressure ratio, 3.0.

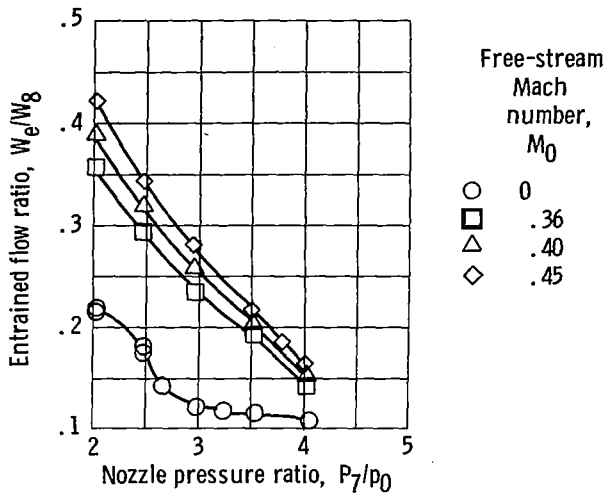

Figure 11. - Entrained ejector flow for two-dimensional ejector plug nozzle.

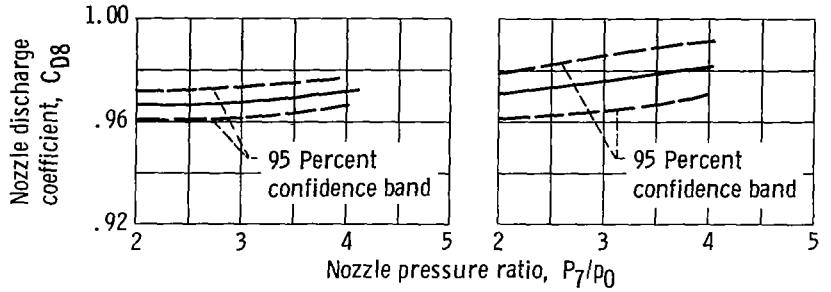

(a) Plug nozzles (without suppressors).

(b) 12-Chute suppressed nozzles.

Figure 12. - Effect of nozzle pressure ratio on two-dimensional nozzle discharge coefficient. Free-stream Mach number, 0 to 0.45.

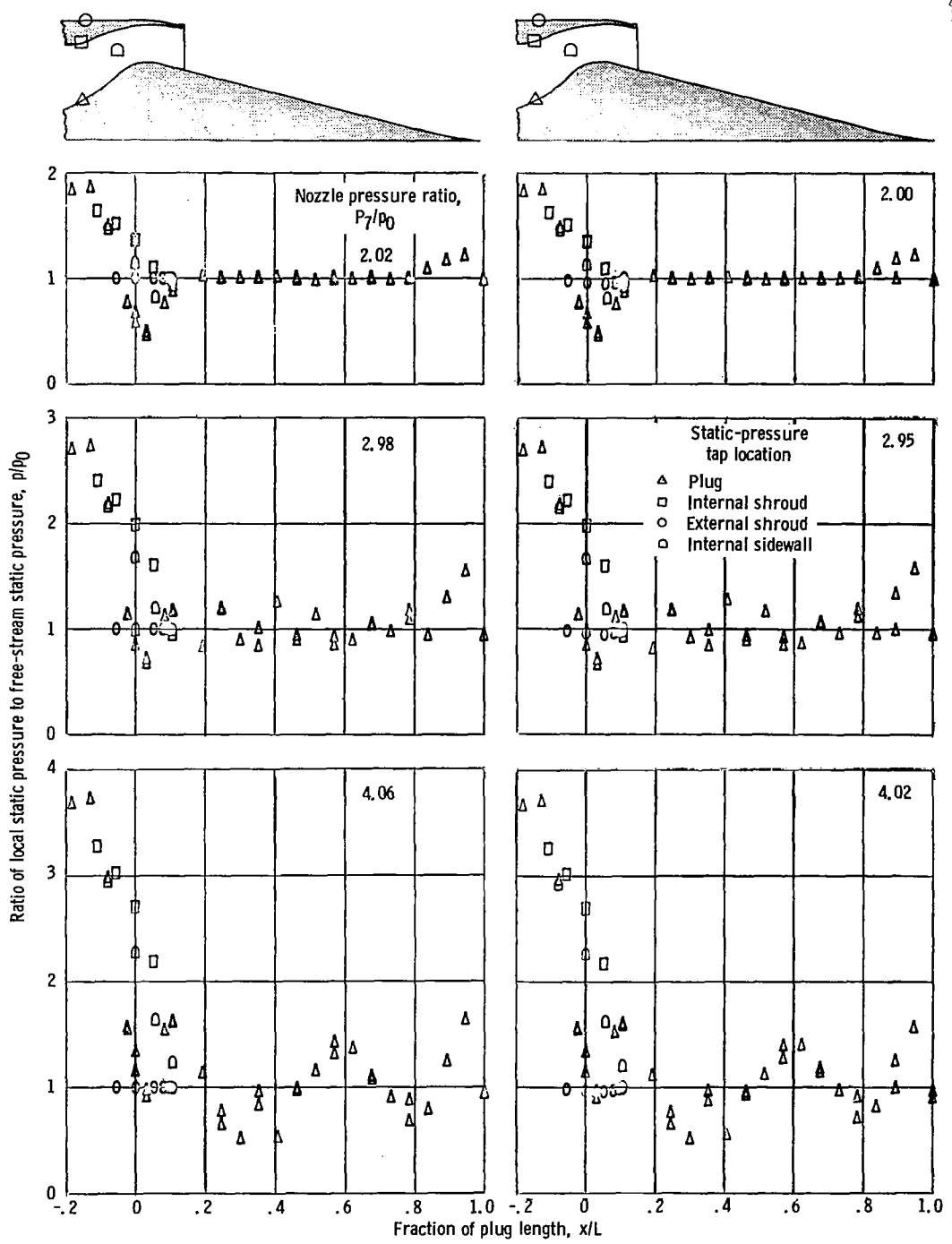

(a) Baseline plug nozzle; free-stream Mach number, 0. (b) Baseline plug nozzle; free-stream Mach number, 0.36.

Figure 13. - Surface pressure distributions for two-dimensional plug nozzles (without suppressors).

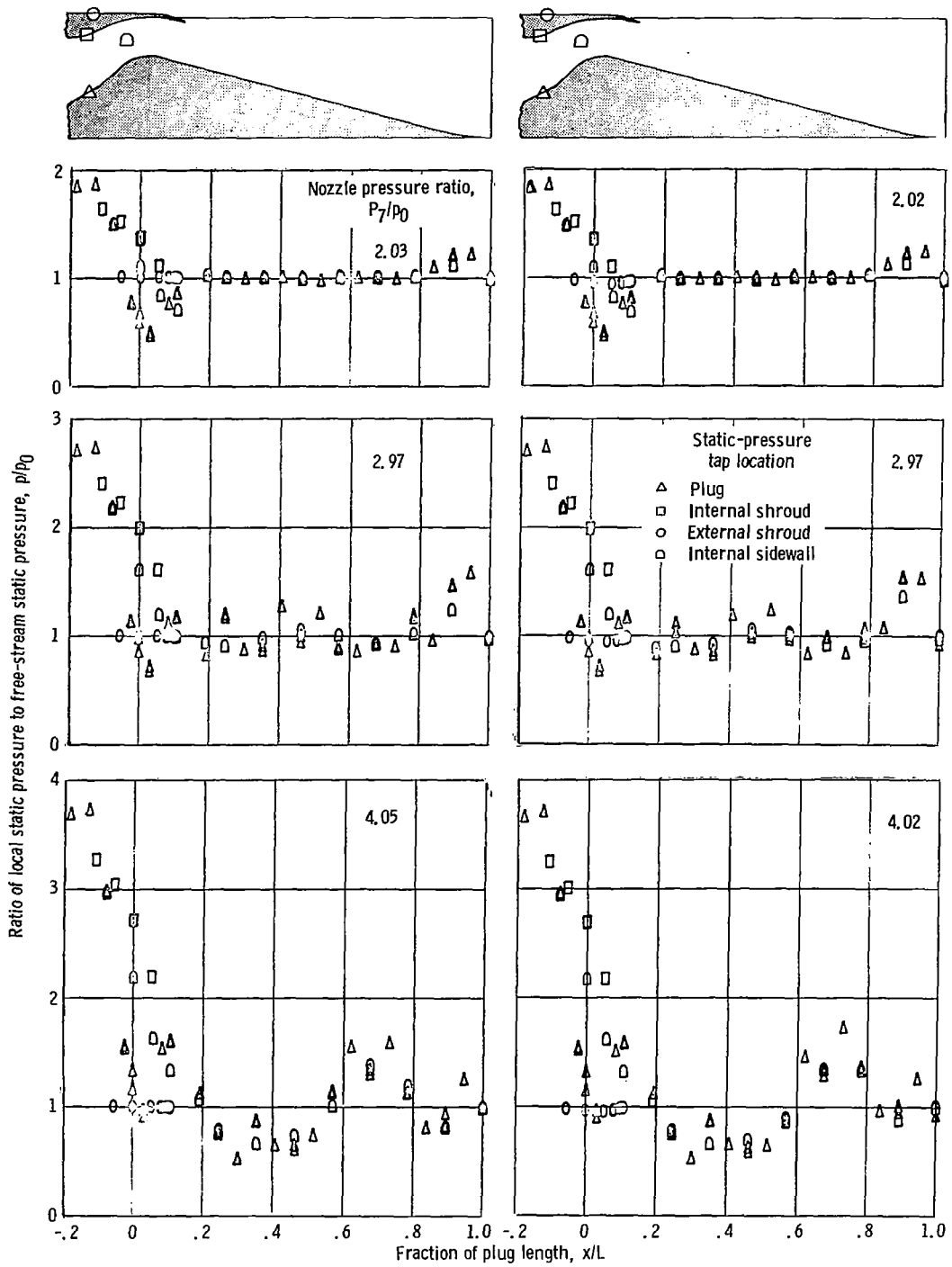

(c) Plug nozzle with sidewalls; free-stream Mach number, 0.

(d) Plug nozzle with sidewalls; free-stream Mach number, 0.36.

Figure 13. - Continued.

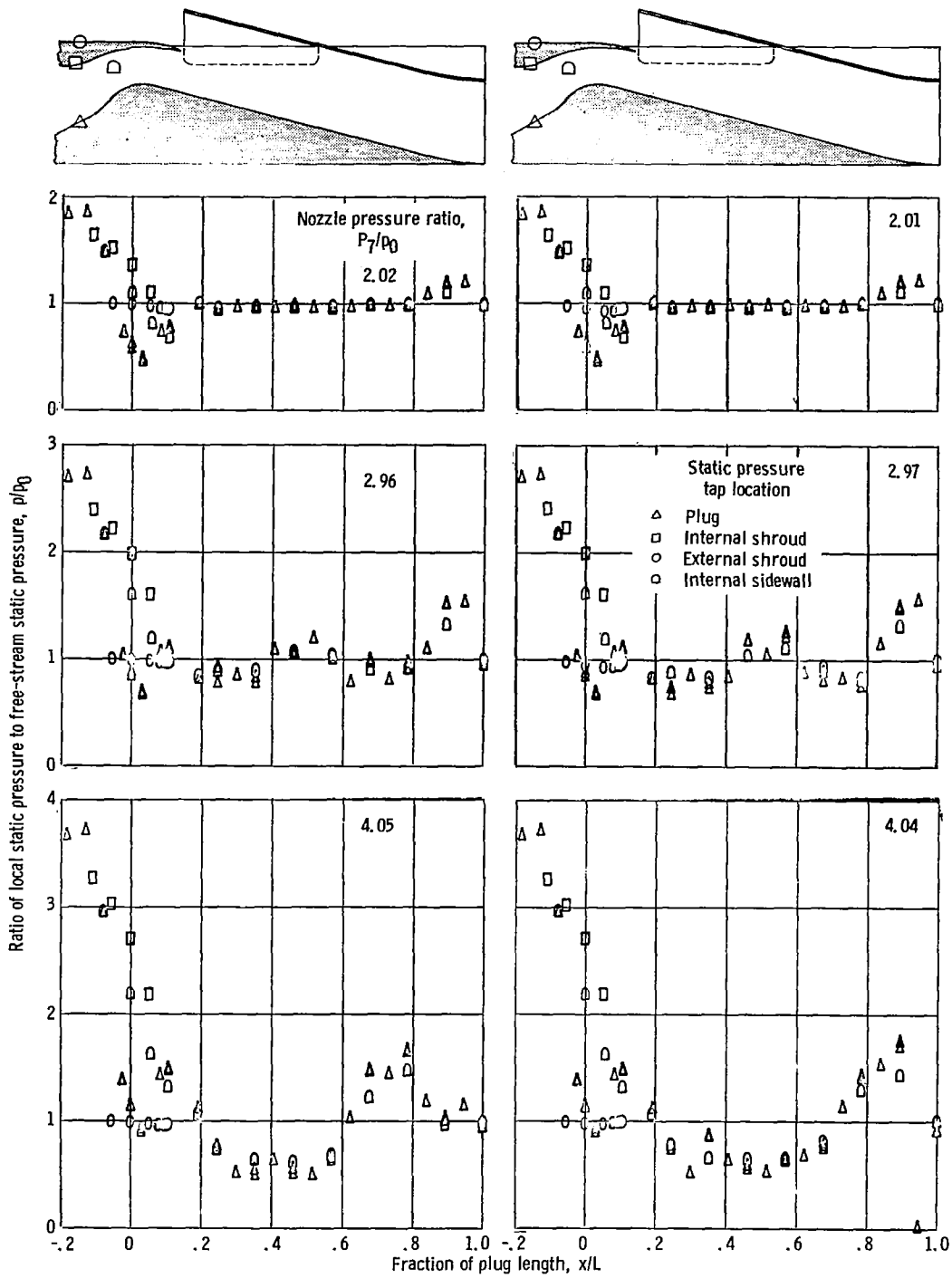

(e) Ejector plug nozzle; free-stream Mach number, 0. (f) Ejector plug nozzle; free-stream Mach number, 0.36.

Figure 13. - Concluded.

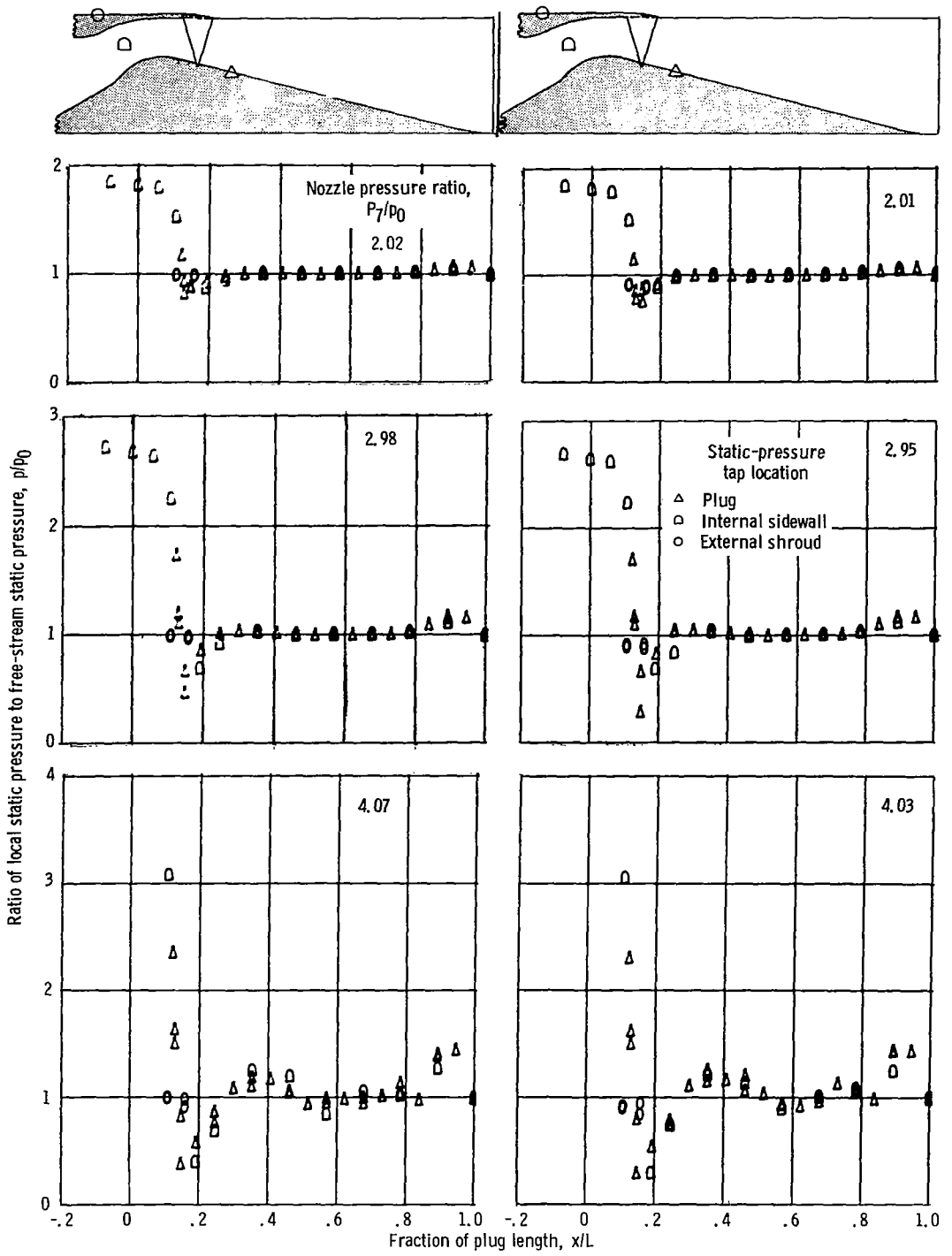

(a) Suppressed nozzle with sidewalls (no slots); free-stream Mach number, 0.

(b) Suppressed nozzle with sidewalls (no slots); free-stream Mach number, 0.36.

Figure 14. - Surface pressure distributions for two-dimensional 12-chute suppressed nozzles.

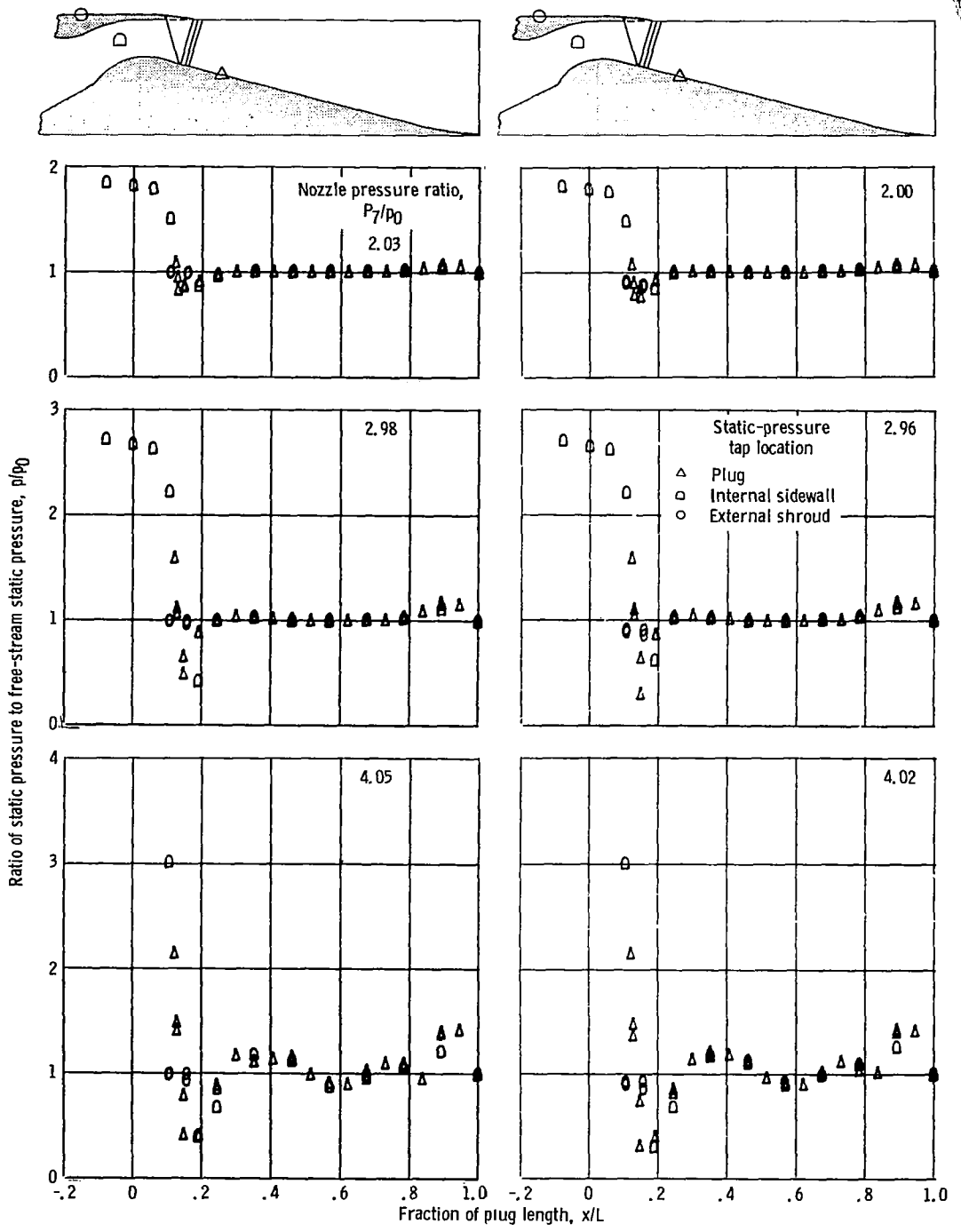

(c) Suppressed nozzle with slotted sidewalls; free-stream Mach number, 0.

(d) Suppressed nozzle with slotted sidewalls; free-stream Mach number, 0.36.

Figure 14. - Continued.

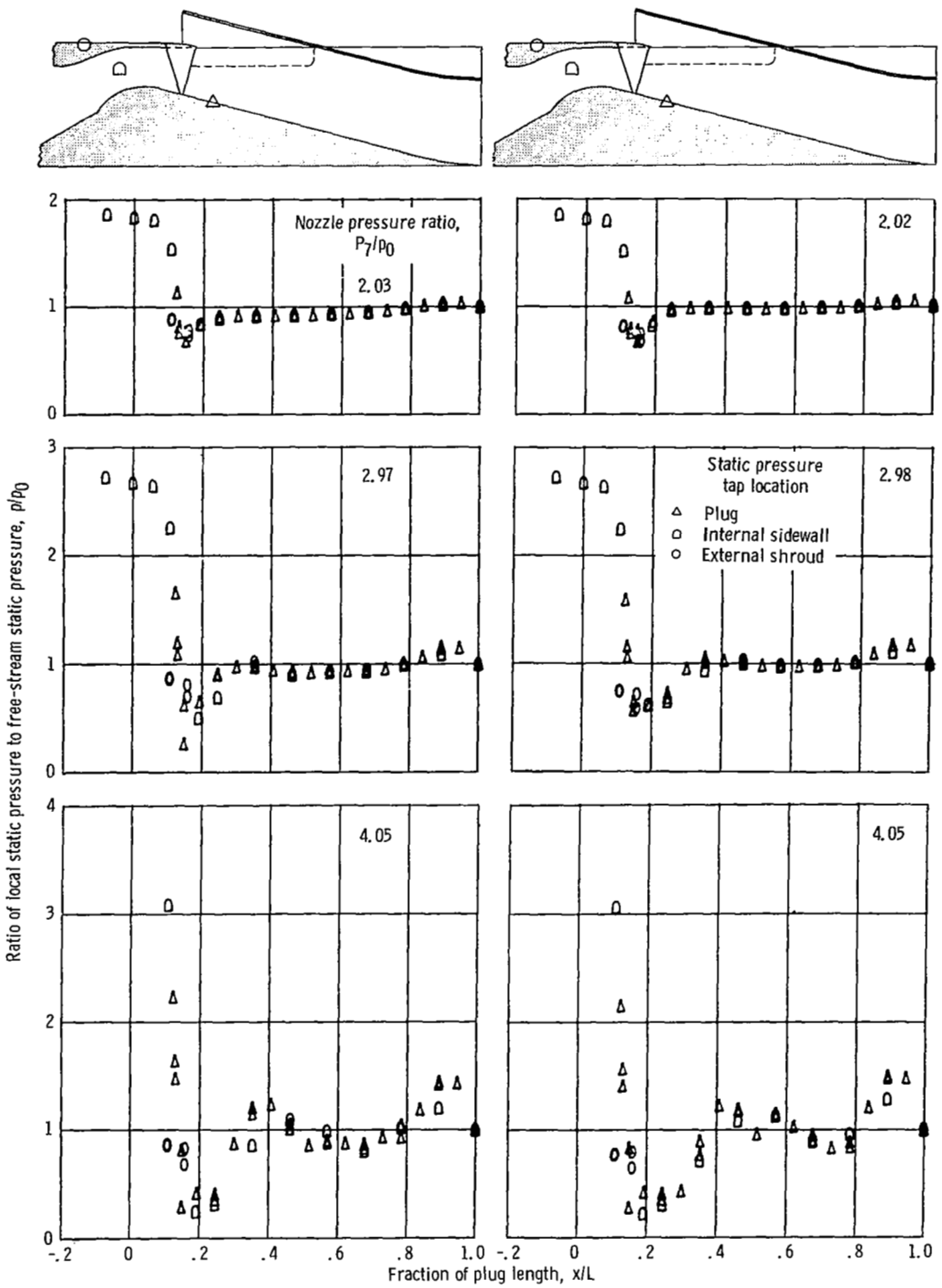

(e) Suppressed ejector nozzle without sidewall slots; free-stream Mach number, 0.

(f) Suppressed ejector nozzle without sidewall slots; free-stream Mach number, 0.36.

Figure 14. - Continued.

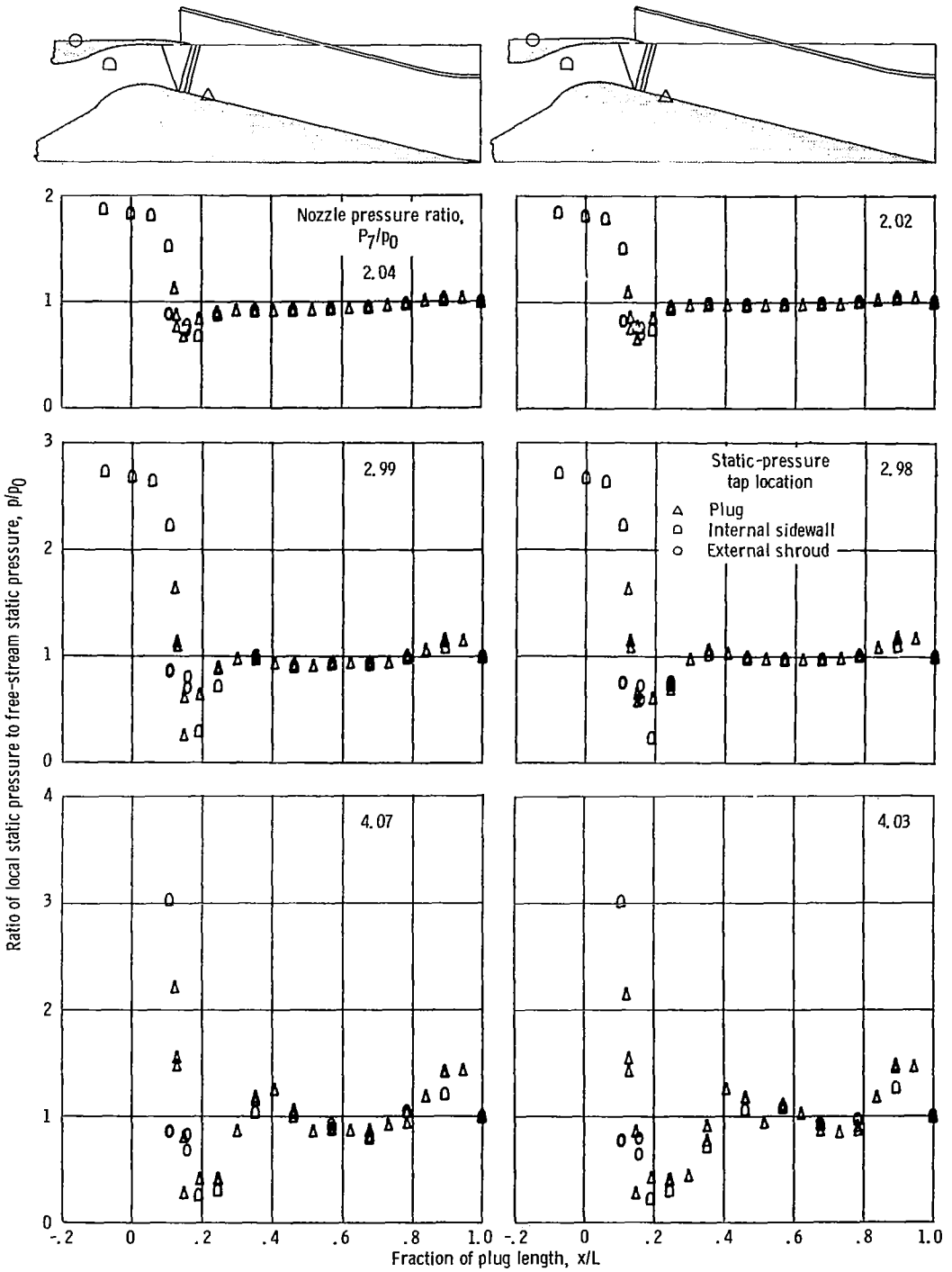

(g) Suppressed ejector nozzle with slotted sidewalls; free-stream Mach number, 0.

(h) Suppressed ejector nozzle with slotted sidewalls; free-stream Mach number, 0.36.

Figure 14. - Concluded.

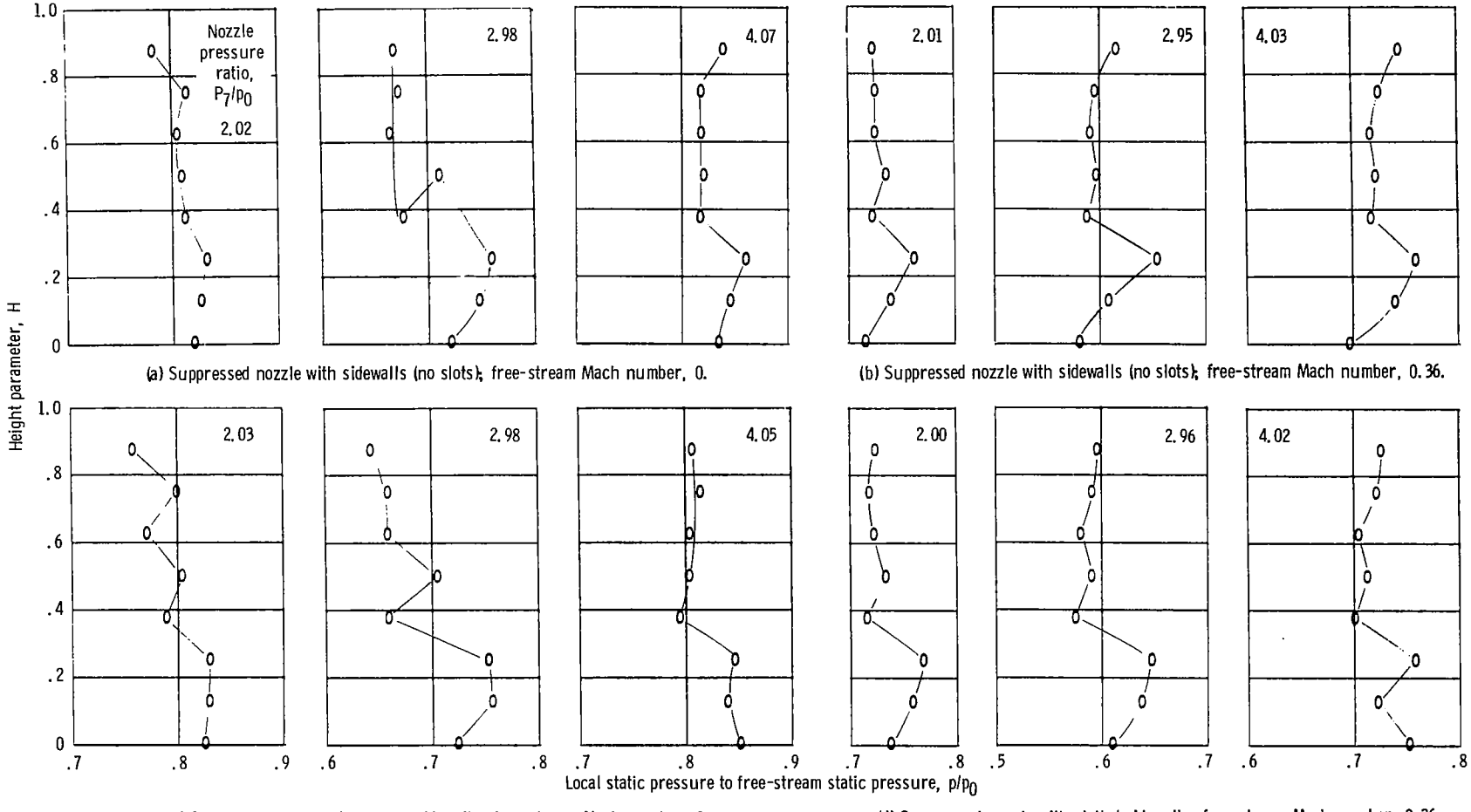

(a) Suppressed nozzle with sidewalls (no slots); free-stream Mach number, 0.

(b) Suppressed nozzle with sidewalls (no slots); free-stream Mach number, 0.36.

(c) Suppressed nozzle with slotted sidewalls; free-stream Mach number, 0.

(d) Suppressed nozzle with slotted sidewalls; free-stream Mach number, 0.36.

Figure 15. - Chute-base pressure distributions for two-dimensional, 12-chute suppressed nozzles.

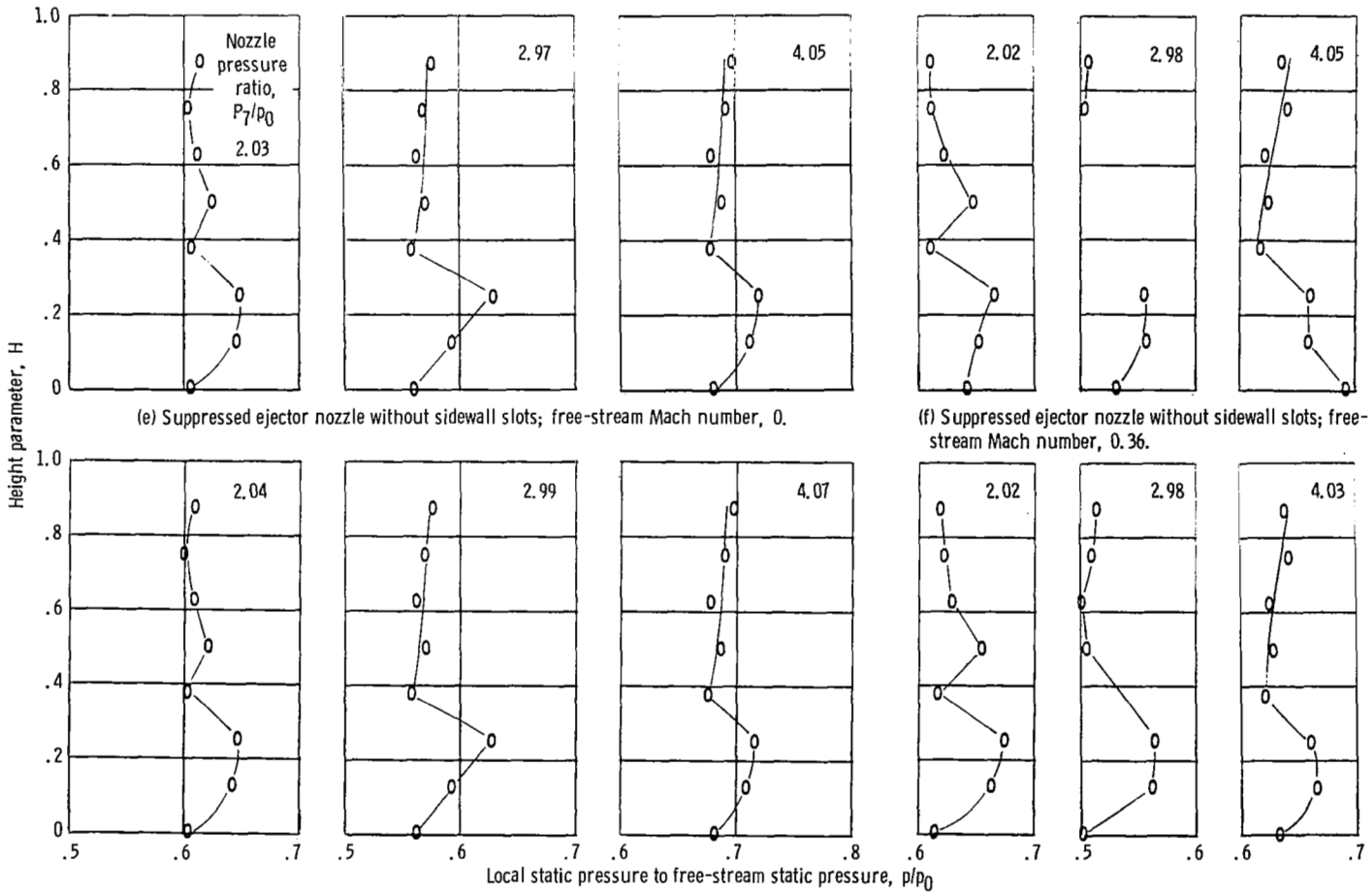

(e) Suppressed ejector nozzle without sidewall slots; free-stream Mach number, 0.

(f) Suppressed ejector nozzle without sidewall slots; free-stream Mach number, 0.36.

(g) Suppressed ejector nozzle with slotted sidewalls; free-stream Mach number, 0.

(h) Suppressed ejector nozzle with slotted sidewalls; free-stream Mach number, 0.36.

Figure 15. - Concluded.

"The aeronautical and space activities of the United States shall be conducted so as to contribute . . . to the expansion of human knowledge of phenomena in the atmosphere and space. The Administration shall provide for the widest practicable and appropriate dissemination of information concerning its activities and the results thereof."

—NATIONAL AERONAUTICS AND SPACE ACT OF 1958

NASA SCIENTIFIC AND TECHNICAL PUBLICATIONS

TECHNICAL REPORTS: Scientific and technical information considered important, complete, and a lasting contribution to existing knowledge.

TECHNICAL NOTES: Information less broad in scope but nevertheless of importance as a contribution to existing knowledge.

TECHNICAL MEMORANDUMS: Information receiving limited distribution because of preliminary data, security classification, or other reasons. Also includes conference proceedings with either limited or unlimited distribution.

CONTRACTOR REPORTS: Scientific and technical information generated under a NASA contract or grant and considered an important contribution to existing knowledge.

TECHNICAL TRANSLATIONS: Information published in a foreign language considered to merit NASA distribution in English.

SPECIAL PUBLICATIONS: Information derived from or of value to NASA activities. Publications include final reports of major projects, monographs, data compilations, handbooks, sourcebooks, and special bibliographies.

TECHNOLOGY UTILIZATION PUBLICATIONS: Information on technology used by NASA that may be of particular interest in commercial and other non-aerospace applications. Publications include Tech Briefs, Technology Utilization Reports and Technology Surveys.

Details on the availability of these publications may be obtained from:

SCIENTIFIC AND TECHNICAL INFORMATION OFFICE

NATIONAL AERONAUTICS AND SPACE ADMINISTRATION

Washington, D.C. 20546